Waveform Analysis of Transmitters of Opportunity for Passive Radar

M A Ringer, G J Frazer and S J Anderson

Surveillance Systems Division
Electronics and Surveillance Research Laboratory

DSTO–TR–0809

ABSTRACT

This report investigates the suitability of a number of broadcast band transmitters of opportunity for a passive radar. Specifically, this report reviews the design of active radar waveforms, measures emissions for representative transmitters of opportunity, and assesses the suitability of these signals for various types of radar observation.

This report shows that it is indeed possible to construct the suggested passive radar, although performance is limited and depends largely on other parameters, such as receiver bandwidth, antenna pattern and observation time.

Published by

DSTO Electronics and Surveillance Research Laboratory
PO Box 1500
Salisbury, South Australia, Australia 5108

Telephone: (08) 8259 5555
Facsimile: (08) 8259 6567

AR No. 010–901
June, 1999

APPROVED FOR PUBLIC RELEASE

Waveform Analysis of Transmitters of Opportunity for Passive Radar

EXECUTIVE SUMMARY

Most radar systems work by actively illuminating the target environment with a specific waveform of appropriate energy and measuring the energy scattered by the target to determine target parameters, such as range, bearing and velocity. Accordingly, most radar systems use a radar waveform that optimises performance and much research has been completed in the field of active radar waveform design.

An alternative is not to deploy a dedicated radar transmitter, but rather to make use of transmissions of opportunity such as radio and television broadcast signals. Transmitterless passive radar has a number of advantages, such as being able to operate without being detected, which makes it more attractive than conventional active radar for certain defence-related missions. It also has disadvantages, one which is that the illumination waveform is almost certainly not optimal for radar operation.

This report investigates the waveforms generated by a number of representative transmitters of opportunity, and shows how these waveforms affect the performance of a passive radar system utilising them. It attacks the problem of opportunistic passive radar with waveform design theory and an assessment of the suitability of the transmissions of opportunity to the matched filter receiver. Previous analysis of this kind has been for very specific radar systems and little work is available which addresses the issues with radar waveform theory.

This report details the requirements for constructing a passive radar and shows how its performance varies as a function of receiver bandwidth, antenna pattern and observation time. The results that this report formulates and the conclusions it draws provide a solid foundation for anyone desiring to construct a passive radar.

Authors

Maurice A Ringer
Surveillance Systems Division

After gaining Bachelor degrees in Electrical Engineering (Hons) and Information Technology from the Queensland University of Technology (QUT), Maurice moved to Adelaide and began work with the Radar Processing and Tracking Group, Surveillance Systems Division, DSTO in 1996. While at DSTO he has been primarily involved with the signal processing behind high frequency over-the-horizon radar (HF OTHR).

During 1997 and 1998 Maurice completed part-time a Masters of Maths Science (Signal and Information Processing) at the University of Adelaide.

Dr Gordon J Frazer
Surveillance Systems Division

Gordon Frazer received the B.E.(Hons) degree from the University of Canterbury, in Christchurch, New Zealand, in 1982; the M.Eng.Sc from the University of Queensland, in Brisbane, Australia, in 1990; and the Ph.D degree from Queensland University of Technology, in Brisbane, Australia, in 1996. From 1982 to 1988, he worked in the Communications Section of the Queensland Electricity Commission, Brisbane, Australia, on various communications problems in the area of electricity transmission. From 1988 to 1990 he was with Mosaic Electronics, Qld., Ltd., Brisbane, Australia, designing real-time digital signal processing hardware and software.

Since 1994, Dr Frazer has been with the Radar Processing and Tracking Group, Surveillance Systems Division, DSTO, where he has been working on various signal analysis problems in high frequency (HF) radar. Dr Frazer's research interests are in the area of signal processing and radar.

Dr Stuart J. Anderson
Surveillance Systems Division

Stuart Anderson attended the University of Western Australia, where he obtained a B.Sc.(Hons) in Physics in 1968, followed by a Ph.D in Physics in 1972, before commencing work at the Weapons Research Establishment, Salisbury (now DSTO). In 1974 he joined the JINDALEE HF skywave 'Over-the-Horizon' radar project trade-off studies team, where he was responsible for studies aimed at developing a ship detection capability for the Stage B radar. From 1977 until 1986 Dr Anderson conducted theoretical and experimental studies of ship detection and remote sensing of the ocean surface. He spent 1986/87 at the US Naval Research Laboratory in Washington DC, followed by a year in the UK at the Admiralty Research Establishment, Portsdown. Since then, as a member of the Radar Processing and Tracking Group in HF Radar Division (now Surveillance Systems Division), he has led research programs across the full spectrum of HF radar-related activities.

Contents

Appendices

Figures

Chapter 1

Introduction

Most radar systems work by transmitting a specific electro-magnetic signal into a region and detecting the wave scattered by an object of interest. By analysing this scattered signal, it is possible to determine information about the object, such as range, bearing, cross-section and velocity. This signal is referred to as the radar waveform, and the ability of the radar to perform these previously mentioned tasks rests heavily upon it.

Accordingly, most radar systems use a radar waveform that optimises performance and much research has been completed in the field of radar waveform design [1–4].

An alternative radar system would be one which uses electro-magnetic signals that are already present in the target environment. This configuration is often referred to as passive radar, as the transmitter is not part of the system.

Requiring no transmitter, passive radar has many benefits, including being typically smaller and more portable, less expensive, requiring less design effort and no shielding or licensing issues (for spectrum allocation). Passive radar could also provide great advantages in defence as the operation of typical active radar is easily detected (the transmitted waveform is very distinct and usually occupies known or easily determined carrier frequencies). For this reason, active radar has the following disadvantages:

- Ships, submarines and planes using active radar for navigation or target detection may find it impossible to travel inconspicuously within particular regions.
- It may prove impossible to use an active radar to inconspicuously monitor a sensitive region of interest.
- Many offensive measures, such as High-speed Anti-Radiation Missiles (HARMs), work by following the enemy's radar transmissions to their source [5].

Transmitter-less passive radar is undetectable and thus presents none of the above limitations.

The concept of utilising transmitters of opportunity is not new, although the majority of available literature considers only the possibility of using illumination provided by another radar. Schoenenberger and Forrest [6] and Green [7] both detected signals from the radar transmitter located at an airport to determine the location of planes arriving

at and departing from that airport. More general investigations of passive radar which utilise transmissions from other radar have been performed by Thompson [8], Munich and Schecker [9] and Lindop [10]. The advantage of such radar systems is that the radar waveform is optimised for target detection and parameterisation.

It is conceivable that a passive radar employ the use of transmissions from more general sources such as radio and television broadcast towers. In this system, the radar waveform would not be optimum, but an effectively random one generated by modulating information such as speech, music and video. Joint research between the University College, London, and Britain's Defence Research Agency [11–13] showed that such a radar was possible using television broadcast transmissions, although performance was very limited. Also, Sahr and Lind [14] demonstrated a radar which utilised transmissions from a local FM radio station to monitor the state of the upper atmosphere. Due to its application to defence, it is believed that much more research has been performed for this class of passive radar than is available in the open literature.

This report investigates the waveforms generated by such transmitters of opportunity, and shows how these waveforms effect the performance of a passive radar system utilising them. The work presented in this report is a generalisation of the work performed by the authors mentioned in the previous paragraph, who have attempted to analyse very specific passive radar systems. This report attacks the problem of opportunistic passive radar with waveform design theory and an assessment of the suitability of the transmissions of opportunity to the matched filter receiver.

This report will show that it is indeed possible to construct the suggested passive radar, although performance is limited and depends largely on other parameters, such as receiver bandwidth, antenna pattern and observation time.

The rest of this chapter completes the introduction to the problem. It outlines the contents of this report and discusses the approximations and assumptions used throughout it.

Chapter 2 presents a brief theory of radar waveforms. The importance of the waveform to radar performance has already been stressed and this chapter explains this relationship. It introduces the matched filter and ambiguity function and gives the reader some appreciation of radar waveform design.

Chapter 3 provides some details on what transmissions of opportunity exist and proposes a radar system which utilises these transmissions. It provides a picture of how a non-cooperative passive radar could be constructed however it is left to the following chapter to determine whether it would work.

Chapter 4 applies the theory of chapter 2 to the proposed system of chapter 3. It shows that the suggested radar could work and details how the other variables of the radar can be adjusted to provide the best possible performance.

Chapter 5 provides a number of simulated examples of the ideas presented in this report. Although many parameters of the radar and environment are simulated, actual waveforms from transmitters of opportunity are used. These simulations provide some confirmation of the results attained in chapter 4 and an initial picture of the performance of the suggested passive radar.

The topic of waveform analysis for passive radar is a vast subject and this report attempts only to be one part of a more detailed investigation. Topics of study which build on the results presented in this report and suggestions on physical implementation of the proposed radar system are given in the concluding chapter of this report.

Chapter 2

Radar Waveform Theory

The ability of a radar to detect targets amongst returns from other objects (clutter) in a region of interest and the ability to determine parameters of these targets, such as range, bearing, size and velocity, depends largely on the radar waveform. This chapter, and the rest of this report, focuses upon the effect of the waveform on the ability to detect targets amongst clutter and determine the range and velocity of these targets. The reason for this is that the accuracy with which the range and velocity may be determined is controlled by the waveform used by a bistatic radar with stationary transmitter and receiver. The ideas presented however, can be simply extended to extract other information about the target such as acceleration and cross-range, which is possible in synthetic aperture radar (SAR).

Provided the wave scattered from the target can be detected, range is proportional to the delay in time between transmission of the waveform and reception of the scattered component, and velocity is proportional to the shift in frequency of the waveform as it is scattered from the target (the Doppler shift). Note that both here and throughout the report, range refers to the total distance from the transmitter to the target to the receiver and velocity refers to the rate of change of this total range. Depending on the location of the transmitter and the receiver and the direction the target is travelling, these parameters may not reflect the actual range and velocity of the target, however it is usually possible to calculate actual range and velocity from the measured values. Chapter 3 details the configuration of the radar being investigated in this report and shows how this conversion would be performed in this case.

It should also be noted that throughout this report the Doppler effect is approximated by a translation in frequency with no distortion to the signal's envelope, that is, $S'(f) = S(f + \alpha)$. The effect on a signal reflected from an object moving at a constant speed however, is actually a scale in frequency and the corresponding envelope scale necessary to conserve energy, that is, $S'(f) = (1/\beta)S(\beta f)$. It can be shown [1] that the above assumption is valid if $(2v/c)T\alpha < 1$, where v is the velocity of the target, T is the radar "look" or integration time, α is the amount of frequency shift and c is the velocity of light. This criteria is readily satisfied throughout this report for the expected values of v, T and α.

The waveforms used in early radars were single frequency sinusoids. These were transmitted either in short pulses in order to accurately measure return time delay or for very

long durations in order to accurately measure Doppler shift. Detection of the scattered wave was ensured to a particular range by adjusting the power in the transmitted waveform. This presented a problem when the desire was to accurately measure range, as the short pulse duration of the waveform required the transmitters to cope with very high peak voltages to attain the required power.

In 1953 Woodward [15] considered using waveforms of more than a single frequency and showed that the ability to detect target range and velocity was actually a function of waveform *shape*, not pulse duration. He laid the foundations for a unified theory which relates the waveform to the ability of the radar both to detect targets and to resolve target range and velocity. It is an overview of this theory which is presented in this chapter.

Usually, this theory is used in waveform design, that is, determining what waveform a radar would use given a specific desired performance. This project proposes to investigate waveforms emitted from transmitters of opportunity, so this ability is not directly important. However, understanding what is necessary in designing a satisfactory waveform is important in determining whether a given waveform will perform satisfactorily.

2.1 Matched filter receivers

Independent of which waveform is used, it is an obvious requirement to extract the most information about the target as possible from the received signal. This involves minimising the inaccuracies due to the various noises which invariably corrupt the received signal.

The receiver which is used by the vast majority of radars and communication receivers is the one which optimally detects the transmitted signal in the presence of additive white Gaussian noise. It is referred to as the matched filter and takes the form:

$$h(t) = s(T - t) \tag{1}$$

Where $h(t)$ is the impulse response of the matched filter, $s(t)$ is the signal desired to be detected and T is the delay of the filter.

This result is derived by maximising the ratio of the probability that the received signal contains $s(t)$ to the probability that it does not, a ratio referred to as the likelihood function. The same result can be determined by maximising the signal–to–noise ratio (SNR) of the output of the filter. This is the method by which North [16] originally derived the above expression. For a detailed derivation of the matched filter the reader is referred to either Cook and Bernfeld [1] (pages 18-33) or Van Trees [17] (pages 275-279).

In the case of radar, the signal to be detected is the component of the radar waveform scattered by the target. As it is desired that the filter optimally detect the signal scattered from a target whose location causes a delay in time τ and whose velocity causes a Doppler shift ϕ of the transmitted waveform $x_o(t)$, then:

$$s(t) = x_o(t + \tau)e^{i\phi t} \tag{2}$$

which implies that the optimum filter is:

$$h(t) = x_o(T - t + \tau)e^{i\phi(T-t)} \tag{3}$$

Note that it is assumed the bandwidth of the waveform is small compared to its carrier frequency. It is for this reason that a frequency shift of $x_o(t)$ can be written as a phase shift.

The output of the matched filter at time T is:

$$\begin{aligned} M(T) &= \int_0^T x_r(\nu) h^*(T-\nu) d\nu \\ &= \int_0^T x_r(\nu) x_o^*(T-(T-\nu)+\tau) e^{-i\phi(T-(T-\nu))} d\nu \\ &= \int_0^T x_r(\nu) x_o^*(\nu+\tau) e^{-i\phi\nu} d\nu \end{aligned} \tag{4}$$

where $x_r(t)$ is the received signal.

The delay required by the matched filter, T, is the radar integration time and will be assumed a constant from this point on. Instead, the output of the matched filter will be expressed as a function of τ and ϕ, which corresponds to the range and velocity of the target which is being tested for detection. Adding a normalising factor, the final expression for the matched filter receiver for radar is:

$$M(\tau,\phi) = \frac{1}{T}\int_0^T x_r(t) x_o^*(t+\tau) e^{-i\phi t} dt \tag{5}$$

In practice, the matched filter is often implemented on a digital computer and $x_r(t)$ and $x_o(t)$ are converted into the digital signals $x_r[n]$ and $x_o[n]$ respectively, where $x[n] = x(nT_s)$ and T_s is the sample period. In this case, the equation for the matched filter receiver is:

$$M(\tau,\phi) = \frac{1}{N}\sum_{n=1}^{N} x_r[n] x_o^*[n+\tau] e^{-i\phi n} \tag{6}$$

where N is the number of samples in the integration time ($T_s N = T$). Issues arising from digitally performing matched filtering are discussed in section 2.5.

The expression for the matched filter receiver can be viewed as a correlation between the transmitted signal, delayed in time by τ and shifted in Doppler by ϕ, and the received signal. For this reason, the matched filter is often referred to as the correlation receiver.

The result of the matched filter receiver, $M(\tau,\phi)$, is a complex number. As it is the magnitude of this quantity which provides the likelihood of a target being present, the following strategy for target detection is usually adopted:

- Using the received signal, $x_r(t)$, a copy of the transmitted signal, $x_o(t)$, and equation (5), calculate $M(\tau,\phi)$.
- Either digitally or using a square-law device, calculate $|M(\tau,\phi)|^2$.

- Compare this quantity to a single threshold, l. A value of $|M(\tau,\phi)|^2$ greater than l indicates the presence of a target with a location and velocity corresponding to a time delay τ and Doppler shift ϕ.

Van Trees [17] showed that if the noise corrupting the received signal is additive white Gaussian, the above strategy provides optimum detection.

Another point of note is that equation (5) resembles the Fourier transform of the product of the signals $x_r(t)$ and $x_o^*(t+\tau)$ and equation (6) resembles the discrete Fourier transform (DFT) of the product of the signals $x_r[n]$ and $x_o^*[t+\tau]$. This is unsurprising as correlating against different frequency shifts is merely convolution in the frequency domain. This operation can be implemented as a product of the two signals in the time domain and the corresponding Fourier transform.

A consequence of this is that equation (6) could be implemented using a fast Fourier transform (FFT) algorithm. In practice, this and other techniques, such as incorporating information about the waveform into the above equations, are usually required for the matched filter to operate in real-time.

Appendix B.1 contains Matlab code which implements the matched filter receiver.

2.2 The ambiguity function

Let $x(t)$ be the radar waveform. If there exists a single target in the region of interest, the received signal is ideally:

$$x_r(t) = \alpha x(t-t_d)e^{-iw_d t} \tag{7}$$

where the time delay t_d is due to the location of the target, the Doppler shift w_d is due to its velocity and α represents the attenuation of the transmitted signal due to path loss and scattering. From equation (5), the result of the matched filter receiver and square-law device is:

$$\begin{aligned}
|M(\tau,\phi)|^2 &= \left|\frac{1}{T}\int_0^T \alpha x(t-t_d)e^{-iw_d t}x^*(t+\tau)e^{-i\phi t}dt\right|^2 \\
&= \left|\frac{\alpha}{T}\int_{-t_d}^{T-t_d} x(t')e^{-iw_d(t'+t_d)}x^*(t'+t_d+\tau)e^{-i\phi(t'+t_d)}dt'\right|^2 \\
&= |\alpha|^2\left|\frac{1}{T}\int_{-t_d}^{T-t_d} x(t')x^*(t'+(\tau+t_d))e^{-i(\phi+w_d)t'}dt'\right|^2 \\
&= |\alpha|^2\,|\chi(\tau+t_d,\phi+w_d)|^2
\end{aligned} \tag{8}$$

where:

$$\chi(\tau,\phi) = \frac{1}{T}\int_0^T x(t)x^*(t+\tau)e^{-i\phi t}dt \tag{9}$$

The function $\chi(\tau, \phi)$ is the ambiguity function. It describes how correlated a signal is with itself delayed in time by an amount τ and shifted in Doppler an amount ϕ. For this reason it is also referred to as the time-frequency autocorrelation function.

When the signal being examined is discrete, the ambiguity function takes the form:

$$\chi(\tau, \phi) = \frac{1}{N} \sum_{n=1}^{N} x[n] x^*[n + \tau] e^{-i\phi n} \tag{10}$$

Appendix B.2 contains Matlab code which implements this equation.

It should be noted that the exact definition of the ambiguity function varies throughout the literature. Often, for example, the term ambiguity function is used to refer to the quantity $|\chi(\tau, \phi)|^2$.

Equation (8) gives some initial insight to the significance of the ambiguity function: that the result of the matched filter receiver, when the signal received is the scattering from a single target, is the ambiguity function of the transmitted signal, scaled and shifted to be centred on the time delay and Doppler shift corresponding to the location and velocity of the target. In order to extend the relationship between the output of the matched filter and the ambiguity function to more complicated scenarios, it is convenient to consider the scatterer distribution.

The scatterer distribution, $S(\tau, \phi)$, is the portion of the transmitted signal energy received at the radar delayed in time by an amount τ and Doppler shifted an amount ϕ. Thus, a target with location and velocity which corresponds to a time delay t_d and Doppler shift w_d of the transmitted signal, causes a peak in the scatterer distribution at (t_d, w_d). The magnitude of this peak corresponds to the amount of energy scattered from the target which, in turn, relates to the radar cross-section (RCS) of the target. Figure 2.1 shows an example of a scatterer distribution.

Ideally, the output of the matched filter would be the scatterer distribution, for it describes all the radar could determine about the environment. The transmitted waveform provides the method by which the radar is able to measure this environment and thus there exists a function of the waveform which acts as a filter between the scatterer distribution and the radar receiver. This function is the ambiguity function and the three are related by [3]:

$$M(\tau, \phi) = \chi(\tau, \phi) \otimes S(\tau, \phi) \tag{11}$$

where $\otimes$ represents 2D convolution.

In this sense, the ambiguity function is analogous to the lens of a camera, which filters the true picture (the scatterer distribution) on its way to the film (the output of the matched filter receiver). By varying the transmitted waveform it is possible to control the type of lens used in the camera, selecting the appropriate lens for the nature of the objects being photographed.

It has been discovered that there exists fundamental properties which any realisable ambiguity function must obey [2, 18]. These are due to factors such as the transmitted signal possessing positive finite energy and that a signal cannot be defined exactly in both time and frequency. The most important of these properties are:

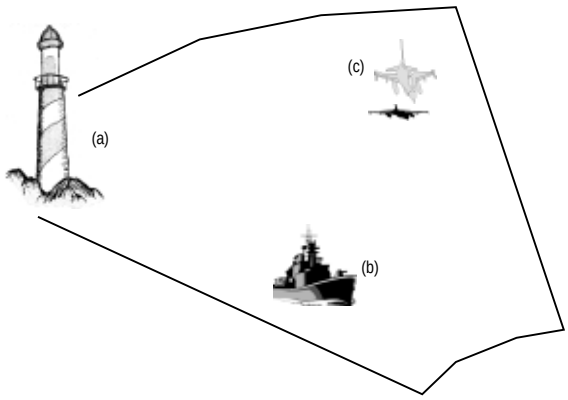

Example region of interest

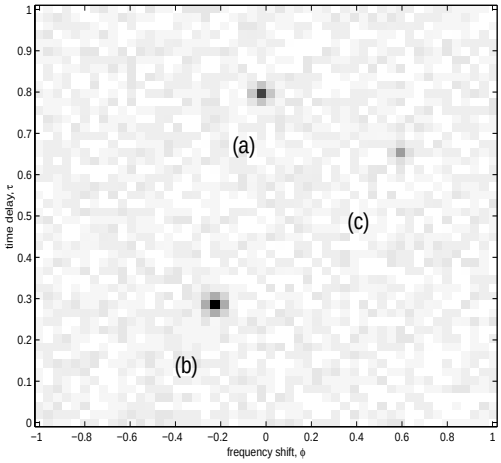

Corresponding scatterer distribution

Figure 2.1: Example of a scatterer distribution. The example targets have the following properties: (a) stationary, medium RCS and furtherest in range, (b) slowly receding, large RCS and closest in range and (c) quickly approaching, small RCS and at medium range.

- A maximum of the magnitude of the ambiguity function always occurs at the origin. That is,
$$|\chi(0,0)| \geq |\chi(\tau,\phi)| \tag{12}$$
- The magnitude of the ambiguity function is symmetric about the line $\tau = \phi$. That is,
$$|\chi(-\tau,-\phi)| = |\chi(\tau,\phi)| \tag{13}$$
- $|\chi(0,0)|^2$ is equal to the amount of energy in the transmitted signal. That is,
$$|\chi(0,0)|^2 = \int_0^T |x(t)|^2 dt \tag{14}$$
- The volume under the surface of $|\chi(\tau,\phi)|^2$ is equal to the square of the energy in the transmitted signal. That is,
$$\int_0^T \int_0^T |\chi(\tau,\phi)|^2 d\tau d\phi = \left[\int_0^T |x(t)|^2 dt\right]^2 \tag{15}$$

These properties limit the choices of possible ambiguity functions and hence possible radar waveforms, which in turn affect how well the matched filter receiver is able to determine the true scatterer distribution. The task of compromising between the effect implied by the ambiguity function and the necessity to maintain the above properties is the essence of radar waveform design and the subject of the following section.

2.3 Resolution issues

It can be seen from equations (8) and (11) that in order to optimally detect a target which produces time delay and Doppler shift parameters t_d and w_d respectively, it is necessary to maximise the value of $|\chi(0,0)|^2$. Also, to minimise the possibility of falsely detecting targets with other parameters, it is necessary to minimise the value of $|\chi(\tau,\phi)|^2$ for $(\tau,\phi) \neq (0,0)$. Thus the ideal radar waveform is one which produces an ambiguity function so that:
$$|\chi_{ideal}(\tau,\phi)|^2 = \begin{cases} 1 & \text{for } (\tau,\phi) = (0,0) \\ 0 & \text{otherwise} \end{cases} \tag{16}$$

Unfortunately, it is impossible for a signal $x(t)$ to produce this ambiguity function. The third and fourth properties of the previous section imply that there must exist a constant volume under $|\chi(\tau,\phi)|^2$ which cannot be confined to the origin, rendering equation (16) impossible to realise.

Thus the ambiguity function must contain volume, or non-zero magnitudes, at values of τ and ϕ away from the origin. When such a function is convolved with the scatterer distribution, three undesirable effects can occur:

- If a large volume of the ambiguity function is located near the origin such as to produce a wide peak there, it may prove impossible to resolve two targets located close to each other (each target will produce a wide peak in the output of the matched filter).

- If the return from one target is significantly larger than the return from another and the location of the second target is such that the peak of the ambiguity function in the matched filter output due to this target lies over a non-zero region of the ambiguity function due to the first target, it is possible that these non-zero values are so large that they mask any return from the second target.
- If values of the ambiguity function away from the origin are large enough, spikes will occur in the output of the matched filter at values of τ and ϕ for which there does not correspond a target. Thus a single target could conceivably produce any number of false detections.

By shaping the ambiguity function it is possible to reduce the possibility of one or two of these effects from occurring, but not all three. If the central spike is narrow enough so that the first effect is avoided, the constant volume requirement implies that the second or third effect is likely to occur. Similarly, the second and third effects can be avoided by concentrating the volume of the ambiguity function to the origin, which provides the first effect.

Some knowledge of the scatterer distribution is required to make a sound judgement on which radar waveform to use. For example, if it is known that all scatterers in the domain of the scatterer distribution have similar RCS, a reasonable radar waveform would be one which produces an ambiguity function with a very narrow spike at the origin and the majority of the volume distributed elsewhere in the (τ, ϕ) plane. Similarly, if the domain of the scatterer distribution is confined to be very small, a possible radar waveform is one which produces an ambiguity function which is zero for a region around the origin. In this case, any false detections due to the non-zero values of the ambiguity function will be associated with targets outside the region of interest.

2.4 Classes of waveforms

Rihaczek [4] argues that any possible radar waveform could be considered a member of one of four classes. Each class has distinct properties and ambiguity function shape.

The first class of waveforms are those for which the product of their duration, T, and bandwidth, B, is approximately unity. The most basic radar waveform, a pulse of single frequency, falls into this class, as does the very narrow, but wideband, impulse function. Such waveforms are designated as Class A waveforms.

The ambiguity function of a Class A waveform consists of a ridge along either the line $\tau = 0$ or $\phi = 0$. Thus these waveforms are able to provide either high resolution in time delay or high resolution in Doppler shift, but not both.

In contrast to Class A waveforms are those signals whose time-bandwidth product is much larger than unity. Such waveforms are often called pulse-compressed signals as they are often generated by passing a single-frequency pulse through a dispersive filter. Waveforms of this type are divided into three classes: Class B1, Class B2 and Class C.

Class B1 waveforms are irregular or noise-like. Typically they are aperiodic and uncorrelated with themselves over any more than a small delay in time or small shift in Doppler.

Thus the ambiguity function of these waveforms consists of a spike at the origin with the bulk of the volume distributed over a low-level pedestal surrounding the spike. Due to their shape, Rihaczek refers to these ambiguity functions as "thumbtack" functions.

Provided the ambiguity function is normalised so that $|\chi(0,0)| = 1$ and that the volume contained in the central spike is negligible, the volume of the pedestal is unity. As with any ambiguity function, those of Class B1 waveforms are confined to the intervals $|\tau| \leq T/2$ and $|\phi| \leq B/2$, so the average height of the pedestal must be $1/(TB)$. This result is summarised in the following equation:

$$\mathrm{E}\{|\chi_{Class\,B1}(\tau,\phi)|^2\} = \begin{cases} 1 & \text{for } (\tau,\phi) = (0,0) \\ \frac{1}{TB} & \text{otherwise} \end{cases} \tag{17}$$

where $\mathrm{E}\{x\}$ refers to the expected value of x.

It will be shown that the waveforms from transmitters of opportunity are Class B1 waveforms. For this reason the ambiguity function of these signals are discussed in more detail in the following chapters, including a more detailed derivation of the above equation in section 4.2.

Due to the shape of the ambiguity function, Class B1 waveforms typically provide good ability to resolve targets in both time delay and Doppler shift, however the location of targets with low RCS are often masked by the pedestal from a target with large RCS.

The third class of waveforms are Class B2 waveforms. Like Class B1 waveforms, these are aperiodic signals with a time-bandwidth product much larger than unity, however Class B2 waveforms are deterministic. They are typically generated by modulating a single frequency pulse with a simple function. A linearly swept FM pulse is an example of a Class B2 waveform.

The ambiguity function of a Class B2 waveform typically consists of a ridge orientated at an angle to the τ and ϕ axis. Thus, it is possible with this waveform to resolve well all targets but those with a Doppler-delay product which matches the angle the ridge is on. For these targets, the ridges produced by the ambiguity functions will align and the exact location of the target on the (τ,ϕ) would be difficult to determine.

Class C waveforms are the final class of waveforms and include all waveforms which are periodic. A periodic signal of period T produces an ambiguity function which is non-zero only for values of ϕ which are multiples of $1/T$ in the same way as the Fourier transform of a signal of period T is a set of lines spaced $1/T$ apart. Also, as the waveform is periodic, the ambiguity function is repeated along the τ axis over the same period T. The result is a set of spikes spaced $1/T$ apart along the ϕ axis and spaced at most T along the τ axis. This shape is often referred to as a "bed of nails".

Class C waveforms thus provide good resolution in both time delay and Doppler shift and are able to resolve targets of greatly varying RCS, however the matched filter output can contain multiple spikes for any single target, thus producing an ambiguity.

Example ambiguity functions of the four classes of waveforms are shown in figure 2.2.

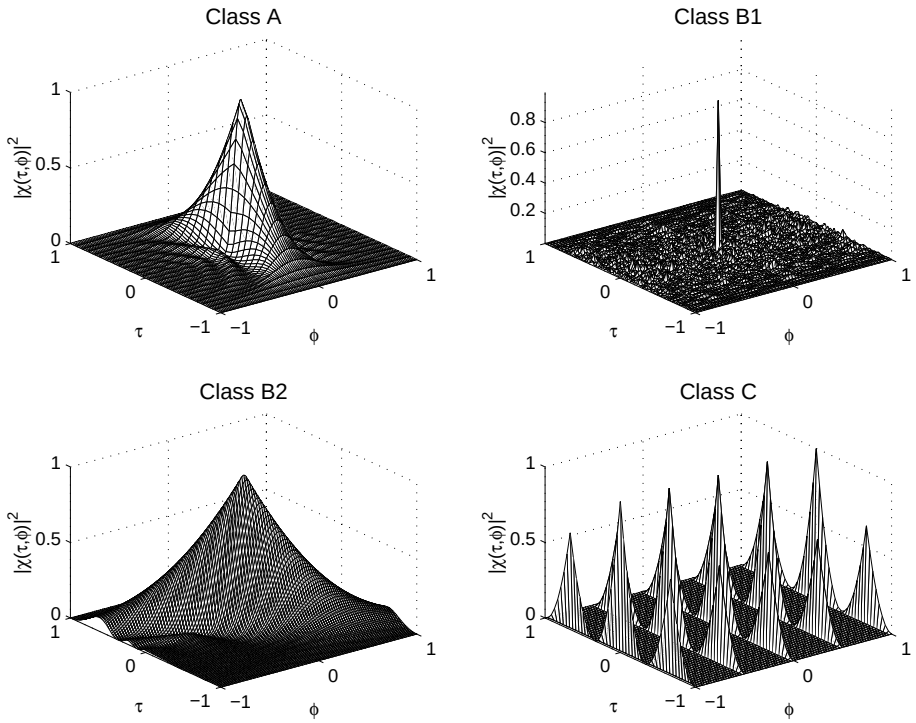

Figure 2.2: Typical ambiguity functions of the four classes of waveforms.

2.5 Implementation issues

The previous sections provide detail on how the shape of the waveform affects how well the radar is able to resolve targets. In practice however, much of the processing is implemented on digital computers and this produces further limits in target resolution.

Equation (6) describes how the matched filter is implemented on a computer. The signals $x_r[n]$ and $x_o[n]$ are the received and original radar waveforms respectively, sampled at the discrete points in time nT_s, where T_s is the sampling period. From this equation it can be seen that it does not make sense to evaluate $M(\tau, \phi)$ for non-integer values of τ, as $x_o[n]$ is not defined for non-integer values of n. This corresponds to being able to compare the received signal with the transmitted one only delayed in time by multiples of T_s.

Also, the fact that the received signal has finite duration, $T = NT_s$ s, implies a degree of smoothness in its spectrum. From Fourier theory is it known that such a spectrum contains independent information only at intervals of $1/T$, so it makes sense to evaluate $M(\tau, \phi)$ only for values of ϕ which correspond to shifts in frequency of multiplies of $1/(NT_s)$ Hz.

Of course, it is possible to evaluate $M(\tau, \phi)$ for values of $\tau \neq kT_s$ and for values of $\phi \neq k/(NT_s)$ (where k is an integer), however the result is merely an interpolation of the values of $M(\tau, \phi)$ which lie on this evenly spaced grid.

This implies that it is not possible to resolve in range targets which produce a signal return delayed less than T_s s apart, nor is it possible to resolve in velocity targets which produce a signal return shifted in Doppler less than $1/(NT_s)$ Hz. This corresponds to

targets no less than cT_s m apart and travelling with velocities different by no less than $c/(NT_s f_c)$, where c is the speed of light and f_c is the carrier frequency of the waveform.

To achieve better range resolution it is required to decrease T_s, the sample period, or rather, increase the frequency at which the radar waveform is sampled. Of course, the radar waveform must have energy at these higher frequencies, which corresponds to Woodward's claim that range resolution is a function of the bandwidth of the radar waveform. To achieve better resolution in velocity it is required to increase $T = NT_s$, the length of radar waveform used by the processor. By increasing the sampling frequency and length of $x_r[n]$ and $x_o[n]$, the grid upon which $M(\tau, \phi)$ can be evaluated becomes finer.

Increasing the sampling frequency or integration time assists the ability to resolve targets in a second way. Usually the received signal, $x_r[n]$, is corrupted with noise and $M(\tau, \phi)$ contains a random component. Increasing the sampling frequency or integration time implies more samples of $x_r[n]$ are being used and the variance of $M(\tau, \phi)$ decreases. If interpolation is used to gain a more accurate estimate of the time delay or Doppler shift of a target, this estimate is improved.

It should be mentioned again that target resolution is a function of both the shape of the waveform and the granularity of this digital grid. It is futile increasing the sample rate or integration time to produce a grid so fine that the width of the peak at the origin of the ambiguity function encompasses hundreds of (τ, ϕ) cells.

Chapter 3

Non-cooperative Passive Radar

This chapter describes the basic elements of a radar which uses the transmissions already present in the region of interest as the radar waveform. The transmitters being utilised are often referred to as non-cooperative since their existence and characteristics are dictated by their own missions rather than by those of the radar.

Section 3.1 outlines the proposed radar configuration which utilises these transmissions. It defines the system which, throughout the remainder of the report, will be investigated for feasibility.

This configuration is clearly bistatic, as the transmitter is located away from the receiver. Section 3.2 discusses some essential principles of bistatic radar, specifically how the parameters gained from the output of the matched filter can be used to determine the actual location and velocity of the target.

Section 3.3 describes what transmissions of opportunity exist. Some initial characteristics of these waveforms are also given, however a more detailed analysis is left for the following chapter.

3.1 Radar configurations

The theory of the previous chapter explains that two signals are required to perform matched filter reception: a copy of the transmitted signal and the received signal. An obvious potential problem of non-cooperative passive radar is that there is no copy of the transmitted signal at the receiver.

To overcome this, it first must be noted that the transmission of opportunity typically arrives at the radar receiver from a specific direction. Usually, this is the direction from the receiver directly to the transmitter, although under certain propagation environments this may not be so.

3.1.1 Two receiver configuration

The first proposed radar system uses two receivers. One receiver (and its corresponding antenna) is fixed to collect the signal arriving at the radar travelling directly from the

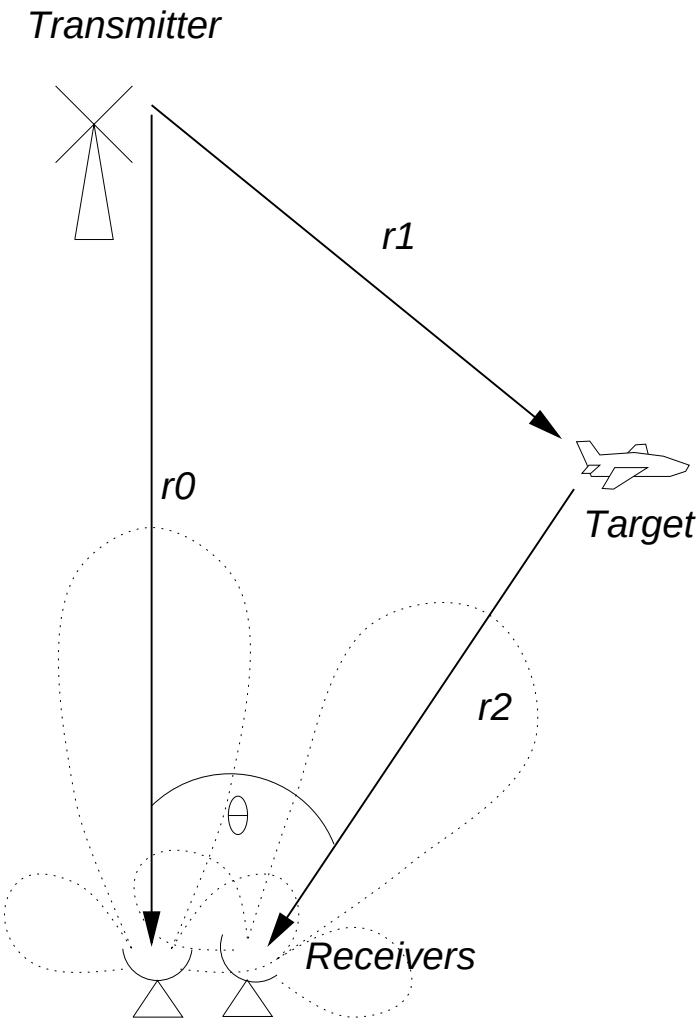

Figure 3.1: Proposed radar configuration.

transmitter of opportunity. This signal will be used as the copy of the transmitted signal and will be referred to as $x_o(t)$. The second receiver and antenna is configured to gather energy from the bearing along which the detection of targets is being attempted. The signal received from this direction will be referred to as $x_r(t)$.

It is important that $x_o(t)$ contain as much of the direct signal and as little of any other signal as possible, and that $x_r(t)$ contain as much of the signal arriving from the direction of interest and as little from any other direction as possible. The responsibility for performing this task falls to the directivity of the antennas and the ability to attenuate signals arriving from directions other than the direction of interest. This concept is illustrated in figure 3.1.

Where this presents the largest problem is at the receiver scanning for target scattering. Typically the energy scattered from a target is less than that in the direct signal, so unless the antenna linked to this receiver attenuates sufficiently in the direction towards the transmitter of opportunity, $x_r(t)$ could conceivably contain more energy from the direct signal than from the scattered signal.

One method for controlling this energy leakage is to use an array of antennas and

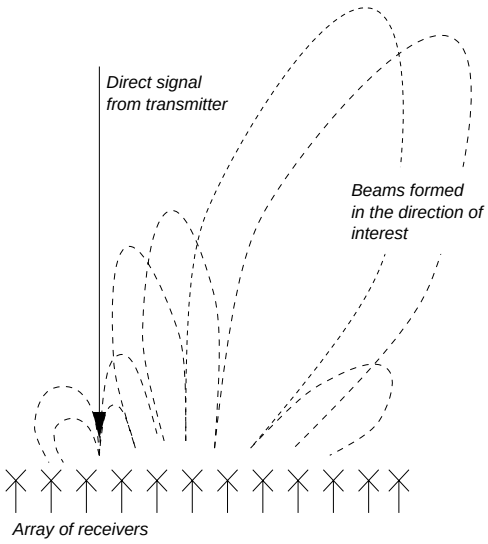

Figure 3.2: Electronically beam-steering with null placement to both scan in multiple directions simultaneously and minimise the energy leaking from the direct signal.

electronically form a beam in the the direction of interest so that a null is placed in the bearing along which the direct signal is arriving. This method also provides the ability to form multiple beams and effectively look in a number of different directions simultaneously. Figure 3.2 illustrates this technique. The study of array processing and beam-forming is a mature field and many procedures have been developed for performing this type of processing [19, 20].

3.1.2 Single receiver configuration

The second passive radar configuration under investigation uses only a single receiver. In this configuration the received signal would contain energy both from the direct signal, $x_o(t)$, and from the scattered signal, $x_r(t)$. It will be shown that for this configuration to be effective, the gain of the antenna in the direction of interest needs to be far greater than that in the direction towards the transmitter of opportunity. The single receiver configuration is illustrated in figure 3.3.

In this configuration, the single received signal is used both as $x_o(t)$ and $x_r(t)$ when performing matched filtering.

3.1.3 Other configurations

For the radar configurations of the previous paragraphs to be able to resolve the location or velocity of the target it is necessary to accurately measure the bearing of the target, θ. To accomplish this for the values of carrier frequency proposed[1], the necessary antennas usually need to be either very large or very complex.

[1] Details of the proposed transmissions of opportunity, including their carrier frequencies, can be found in section 3.3

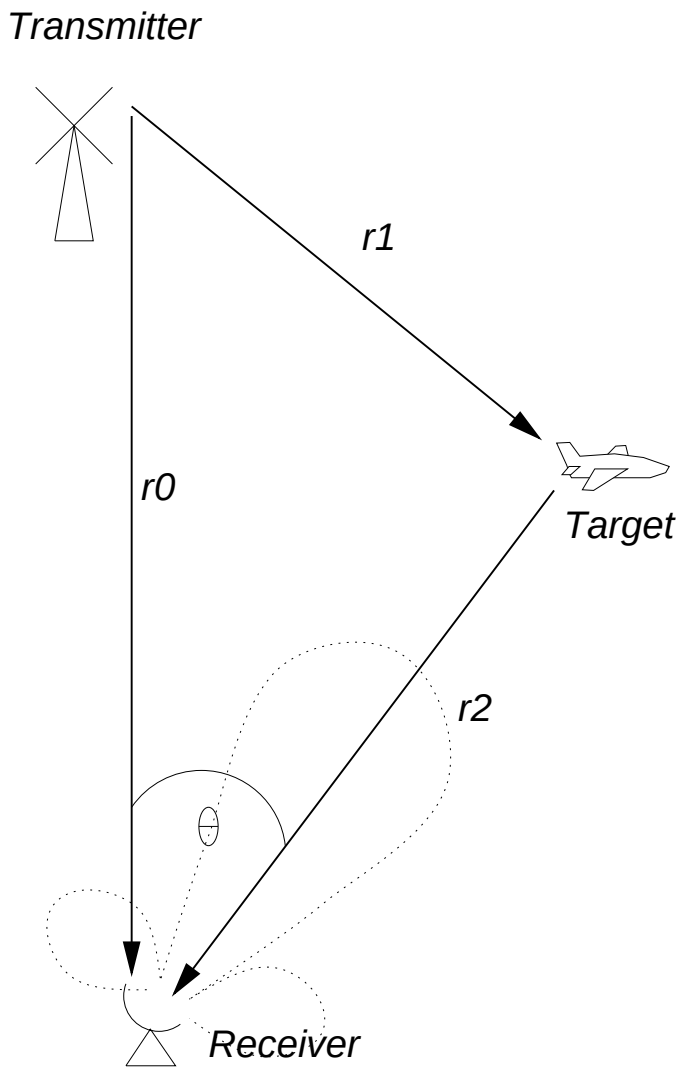

Figure 3.3: Configuration of the passive radar using a single receiver.

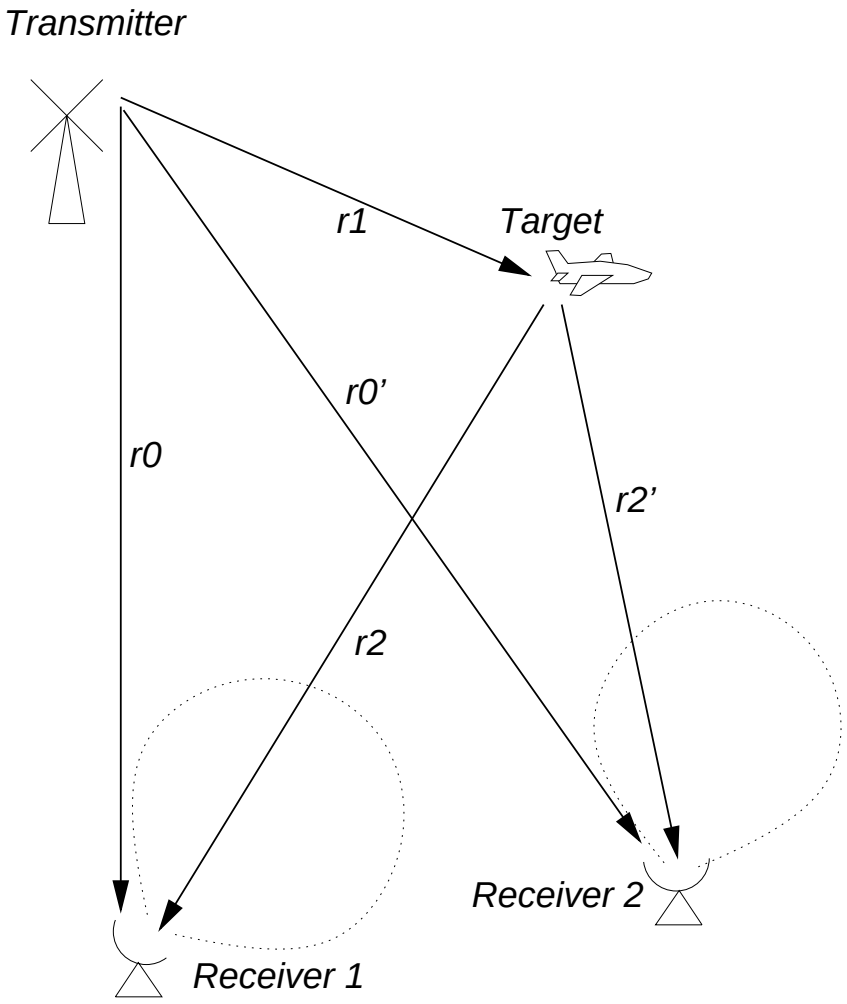

Figure 3.4: Configuration of the passive radar using a two receivers located apart.

A third proposed passive radar configuration involves two receivers located far apart, each using antennas which provide poor resolution in direction, but are still capable of heavily attenuating the signal arriving from the direction of the transmitter of opportunity. Such antennas are typically small and inexpensive to produce. The proposed configuration is illustrated in figure 3.4.

In this configuration, each receiver performs its own matched filtering using the single signal in the exactly the same manner as the receiver in the single receiver configuration. In this system however, direction of the scattered signal, θ, is unknown and the location and velocity of the target is resolved using the second receiver.

Another possible configuration involves utilising more than one transmitter of opportunity. This multi-static arrangement would consist of a number of receivers and corresponding antenna, each configured to one of the three previously proposed configurations. Each receiver would perform its own matched filtering, the results of which would then be combined in some manner to provide a single estimate of the number of targets present, their location and their velocity.

3.2 Bistatic considerations

Chapter 2 showed that matched filter processing provides information on how much the signal scattered from a target is delayed in time and shifted in Doppler. The conversion between the signal delay, t_d, and frequency shift, w_d, produced by a target and the target's actual location and velocity depends on the configuration of the radar. This section examines this conversion for the systems proposed in the previous section.

Figures 3.1 and 3.3 illustrate the dual and single receiver configurations proposed to utilise transmissions of opportunity. It is assumed that θ and r_0 are known, so in order to determine the location of the target, only the the distance r_2 is required, which is given by:

$$r_2 = \frac{ct_d(ct_d + 2r_0)}{2\left(ct_d + r_0(1 - \cos\theta)\right)} \tag{18}$$

where c is the speed of light.

The velocity of the target, v, and direction the target is travelling, θ_v, are given by:

$$v = v_{r1}^2 + v_{r2}^2 + 2v_{r1}v_{r2}\cos(\theta') \tag{19}$$

and

$$\theta_v = \arcsin\left[\frac{v_{r1}}{v}\sin(\theta')\right] \tag{20}$$

where

$$\begin{aligned}
v_{r1} &= \text{target's velocity in the direction of } r_1 \\
&= \frac{r_2}{r_1 + r_2}\left(\frac{cw_d}{2\pi f_c} + r_0 r_2 \frac{d\theta}{dt}\sin\theta - r_0\cos\theta\right) && (21)\\
v_{r2} &= \text{target's velocity in the direction of } r_2 \\
&= \frac{-r_1}{r_1 + r_2}\left(\frac{cw_d}{2\pi f_c} + r_0 r_2 \frac{d\theta}{dt}\sin\theta - r_0\cos\theta\right) && (22)\\
\theta' &= \text{angle between } r_1 \text{ and } r_2 \\
&= \arcsin\left[\frac{r_0}{r_1}\sin\theta\right] && (23)\\
r_1 &= r_0 - r_2 + ct_d && (24)
\end{aligned}$$

and f_c is the carrier frequency of the radar transmission. The angle θ_v is measured relative to the direction towards the target. For example, if the target is travelling directly away from the radar, $\theta_v = 0$. The derivation of equations (18) through (24) can be found in appendix A.

Note that unlike monostatic radar, the ability to measure the range of the target, r_2, is a function of the bearing to it, θ, which may prove difficult to measure accurately. Also, the ability to accurately measure the target's velocity depends on the ability to accurately measure its range (equations (19) and (20) are functions of r_2). This implies the ability to resolve well both the delay in time, t_d, and the Doppler shift, w_d, caused by the target.

Often these inaccuracies can be minimised by using a number of observations and an adaptive or block-based processing technique with the objective of optimally estimating

the target location and velocity against a defined criteria (such as least square error). The radar proposed by Howland [13] used such a method for resolving target location using a number of observations of Doppler shift, w_d, as the waveform used was such that time delay, t_d, was not able to be measured accurately.

Techniques for optimal parameter estimation are well developed and the reader is referred to Anderson and Moore [21] for more information.

Up to this point, it has been assumed that the location of the transmitter of opportunity is known. This is usually the case, as the location of radio and television broadcast towers are readily attainable. If however, these details are not available, they are simply calculated using two receivers located apart. Each receiver scans for the direction from which the strongest signal arrives. Typically, this is the direct signal and lines drawn from each receiver outwards in this direction will bisect at the location of the transmitter.

For a more detailed discussion on the implications of bistatic radar, including equations for resolving target location and velocity for more complex scenarios than those described above, the reader is referred to Skolnik [22] or Willis [23].

3.3 Waveforms of opportunity

The electromagetic spectrum is abundant in signals which arise from numerous sources such as commercial broadcasting stations, private and government radar transmitters and various communications systems. Of these, this report proposes to investigate the following transmissions for their suitability to passive radar[2]:

- **AM radio**
  - Commercial broadcast radio:
    Signals of up to 20 kHz bandwidth occurring at frequencies between 530 kHz and 1605 kHz (wavelengths of 187 m to 566 m)
  - Medium wave and short wave radio:
    Signals of up to 15 kHz bandwidth occurring at various frequencies between 1605 kHz and 26.9 MHz (wavelengths of 11 m to 187 m)
- **FM radio**
  - Commercial broadcast radio:
    Signals of up to 75 kHz bandwidth occurring at frequencies between 88 MHz and 108 MHz (wavelengths of 2.8 m to 3.4 m)
  - Other frequency modulated communications originating from a variety of sources such as land, sea and air mobile communications equipment and satellite transmissions
- **Television broadcasts**
  Signals of up to 6 MHz bandwidth occurring at the following frequencies:

[2]Details of frequencies and bandwidths used in this list come from [24].

- Channels 0-4:
  46.25 MHz to 95.25 MHz (wavelengths 3.1 m to 6.5 m)
- Channels 6-11:
  175.25 MHz to 216.25 MHz (wavelengths 1.4 m to 1.7 m)
- UHF channels:
  527.25 MHz to 814.25 MHz (wavelengths 0.4 m to 0.6 m)

The characteristic which distinguishes these transmissions is that they are all random aperiodic signals. They are generated from random information such as speech, music and video, and modulated using one of three schemes: frequency modulation, amplitude modulation or television's vestigial sideband modulation.

This random information is typically uncorrelated with itself over any more than a small delay in time or shift in frequency. Plain speech, for example, is uncorrelated with a copy of itself delayed any more than 10 ms [25].

The modulation applied to these signals modifies this structure. For the three schemes mentioned above, the modulation causes the energy in the original signal to be distributed over a wider range of frequencies and in the case of frequency modulation, to be distributed more evenly across these frequencies. Thus, provided the pass-band of the receiver is smaller than the bandwidth of the signal produced by this modulation, the spectrum of the received signal contains energy distributed more evenly across all retained frequencies, and thus is uncorrelated with itself delayed over even smaller shifts in time and frequency, than the original signal.

This concludes that the received signal of opportunity is not unlike bandlimited white noise. This assumption is strengthened when the receiver scans for long periods of time and any underlying structure of the signal due to the nature of the transmission is averaged out.

This characteristic is most apparent in the ambiguity function of these signals. Section 2.4 showed that the ambiguity function of a random signal contains a spike at $(\tau, \phi) = (0, 0)$ surrounded by a constant pedestal of energy. Figure 3.5 shows the ambiguity function of an example transmission of opportunity. The signal used to generate this figure was taken from taken from a local FM radio station.

The similarity between the ambiguity function for Class B1 waveforms, shown in figure 2.2, and figure 3.5 confirm that waveforms from the transmitters of opportunity being investigated fall into Rihaczek's second class of waveforms.

The similarity between the transmission of opportunity and white noise breaks down as the bandwidth of the receiver approaches the bandwidth of the transmission of opportunity. The result is that the amount of time and frequency shift required before the signal is uncorrelated with itself increases and the spike in the ambiguity function at $(\tau, \phi) = (0, 0)$ becomes wider.

As the ability to resolve targets is a function of the width of the spike at the origin of the ambiguity function, it is desired to maintain this similarity to white noise, however it is also desired to use a signal of large bandwidth so that the width of a cell along the ϕ axis is kept to a minimum (as explained in section 2.5).

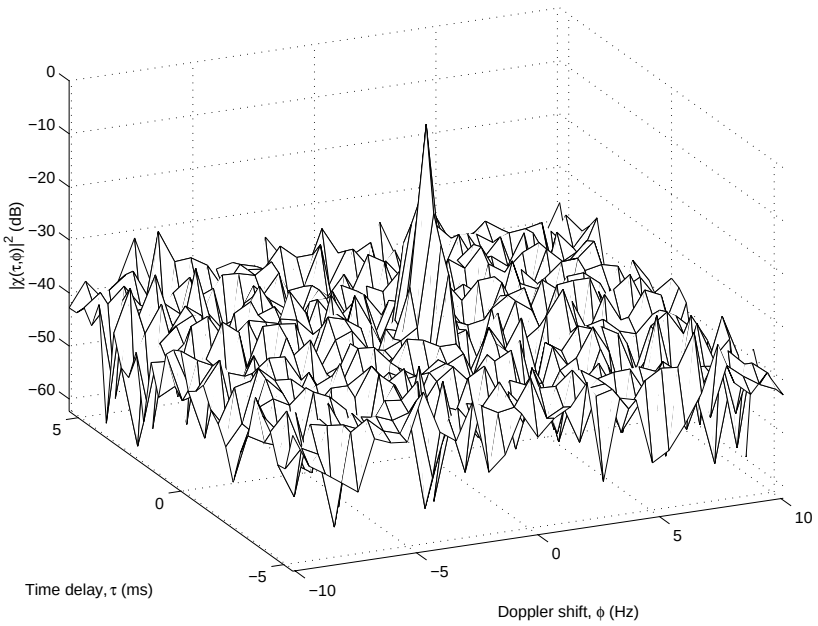

Figure 3.5: Ambiguity function from an example transmission of opportunity. The 3 s long example signal was captured from a local FM radio broadcast using a receiver which had 4 kHz bandwidth.

Further discussion on the characteristics of the transmissions of opportunity requires knowledge of the individual modulation schemes. The remainder of this section discusses the effect of these three schemes.

3.3.1 AM radio

Amplitude modulation produces the signal with the smallest bandwidth of the three types of transmissions being investigated. It also produces the signal which contains the most spectral variance over the same amount of bandwidth. Thus, it is least capable of being modelled by white noise and would most likely make for the worst radar waveform.

More than half of the energy of an AM transmission is contained in the carrier. Most of the remaining energy resides between the frequencies f_c+100 and f_c+3000 Hz and between f_c-100 and f_c-3000 Hz, where f_c is the frequency of the carrier. This distribution of energy results in the received signal being not as white as those produced by the other modulation schemes and the corresponding ambiguity function not containing as distinct a peak at the origin.

An example of the ambiguity function of a typical AM radio transmission is shown in figure 3.6. In this example, the modulation has not removed the underlying harmonics and structure contained in the original signal (which was plain speech) and the relatively large bandwidth has been able to capture this. This effect is evident in the large peaks which are located away from the origin in the ambiguity function.

Obviously, this effect is undesired in a radar waveform. As mentioned in section 2.3, these peaks could mask smaller targets or produce false detections.

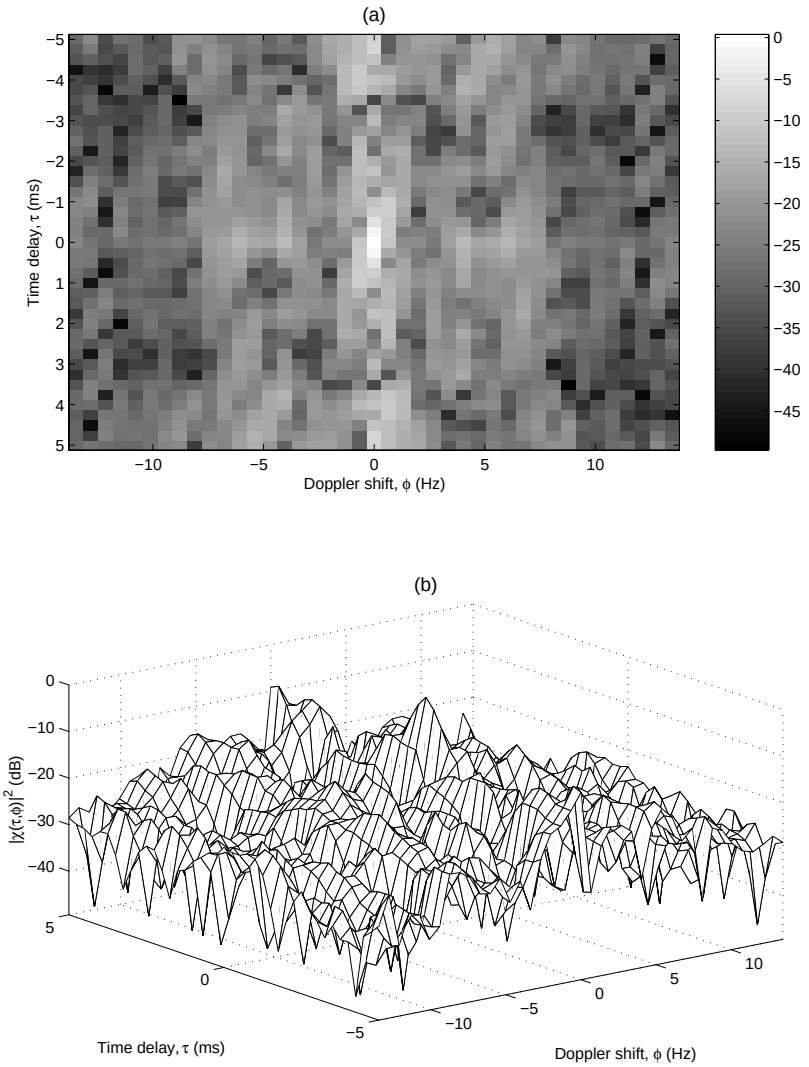

Figure 3.6: Image (a) and mesh (b) view of the ambiguity function of an example AM radio transmission. The example signal was 0.7 s long and supported a 4 kHz bandwidth.

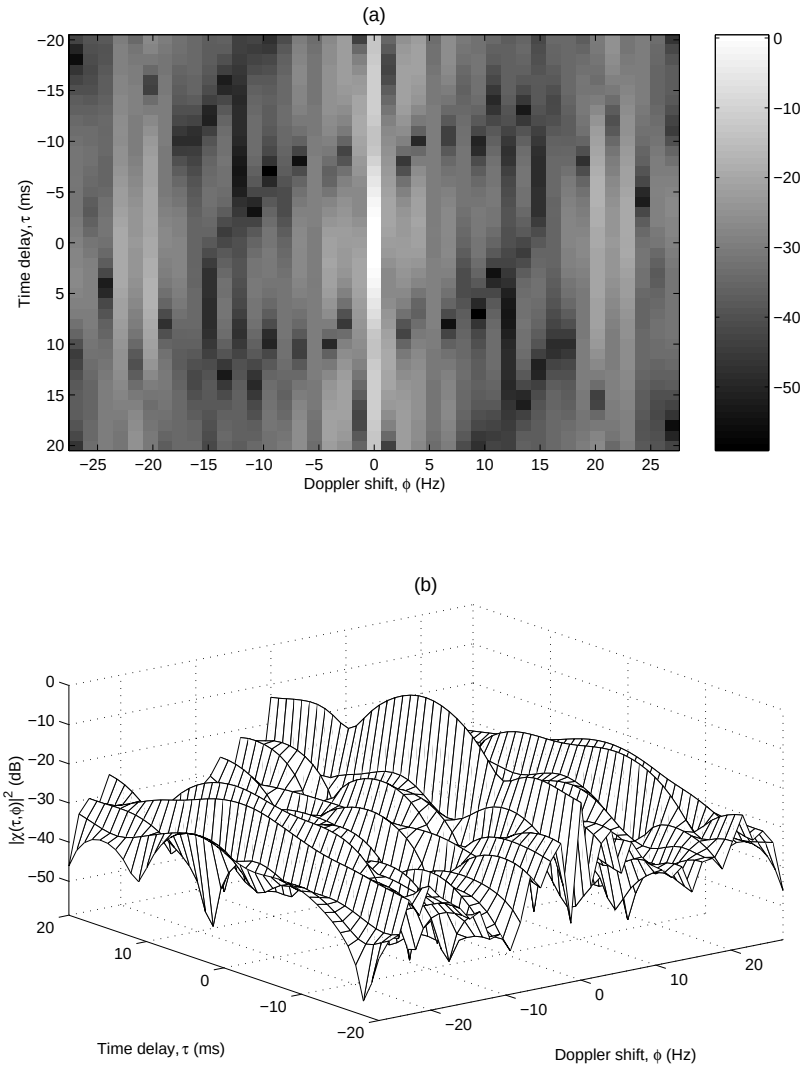

Figure 3.7: Image (a) and mesh (b) view of the ambiguity function of an example AM radio transmission. The example signal was 0.7 s long and was limited to a 1 kHz bandwidth.

One method to improve the shape of this ambiguity function is to take a longer time sample, which would result in the harmonics or structure to be averaged out.

Another method of attempting to shape the waveform into a more usable form is to use a smaller bandwidth. This has the effect of moving the energy of the ambiguity function into the centre however also causing this centre peak to stretch along the τ axis. An example of the ambiguity function of the same signal used in figure 3.6, passed through a filter to limit its bandwidth to 1 kHz, is shown in figure 3.7.

The extreme of this technique is a receiver whose bandwidth is so narrow that $x_o(t)$ effectively consists of a single frequency and the ambiguity function looks like a ridge along the τ axis, like class A waveforms from section 2.4.

3.3.2 FM radio

Frequency modulation produces a signal much closer to the desired bandlimited white noise model than does amplitude modulation, and over a wider bandwidth. The spectrum of an FM radio transmission extends for 75 kHz with the energy being well distributed across most of this bandwidth.

Figures 3.8, 3.9 and 3.10 show the ambiguity functions of example FM radio transmissions. In each figure, a different signal was being modulated and transmitted: figure 3.8 shows the ambiguity function of an FM transmission of rock music, figure 3.9 of classical music and figure 3.10 of plain speech. It can be seen that there is not a lot of variation between the three ambiguity functions, although frequency modulated plain speech appears to provide the finest resolution of Doppler shift (figure 3.10 contains the narrowest ridge).

3.3.3 Television broadcasts

The modulation scheme used for television broadcasts is slightly more complex than that used for AM or FM radio[3]. Three signals are coded together over the 6 MHz bandwidth used by the transmission: a chrominance signal, a luminance signal and the sound track. Mixed with this however, are a number of pulses used by the receiving equipment to determine various synchronising information. The most dominant of these is the line sync pulse.

The line sync pulse is 4.7 μs long, occurs every 64 μs and has an amplitude at least 132 percent of any other information in the television broadcast. For this reason it is expected that the ambiguity function of a television broadcast contains narrow ridges extending $\pm 1/4.7\mu s = \pm 213$ kHz in the ϕ dimension repeated every 64 μs in the τ dimension.

Thus the return from a single target produces any number of returns, each separated along the τ axis by 64 μs. If the region of interest is small enough, this ambiguity may cause no problem.

This effect is also removed if the bandwidth of the receiver is too small to detect this 15,625 times-a-second pulse. When received using filter bandwidths smaller than 15 kHz, the transmission appears to follow closely the desired white noise model. However, as mentioned in chapter 2, there are disadvantages of using smaller bandwidths. Figure 3.11 shows the ambiguity function from a typical television broadcast taken using a receiver which had a 4 kHz bandwidth.

[3] Details of the modulation scheme used by television comes from [26].

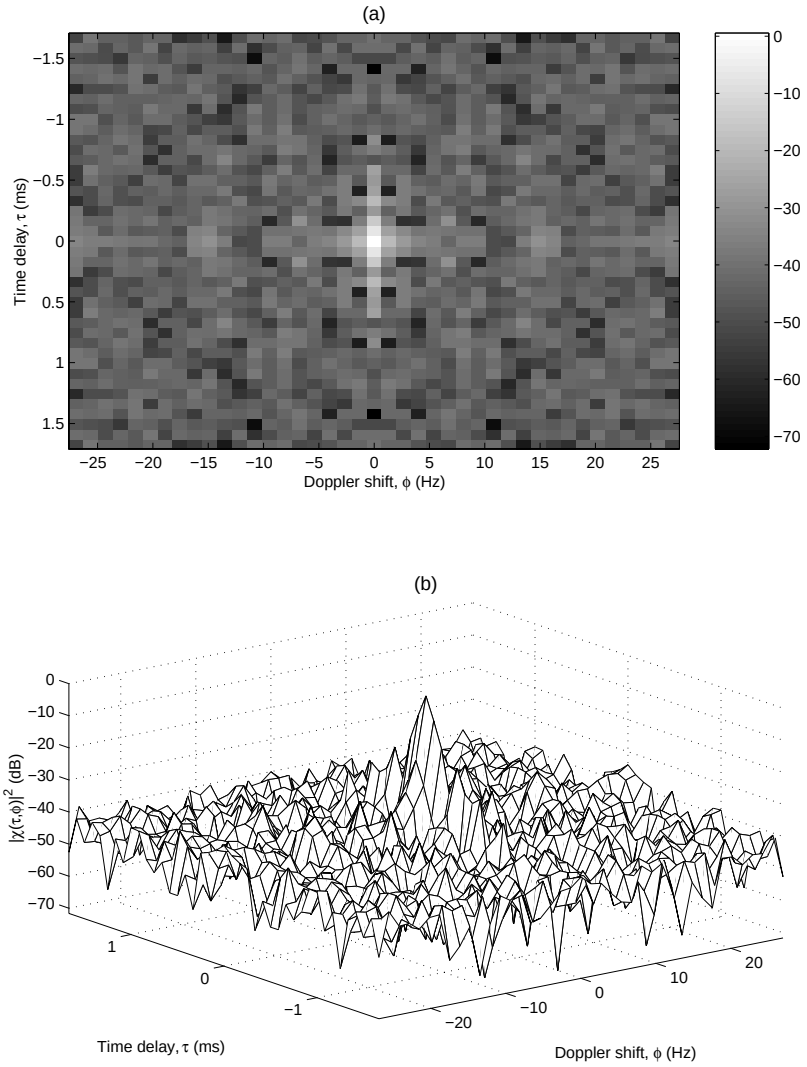

Figure 3.8: Image (a) and mesh (b) view of the ambiguity function of an example FM transmission of rock music. The example signal was 2.7 s long and supported a 12 kHz bandwidth.

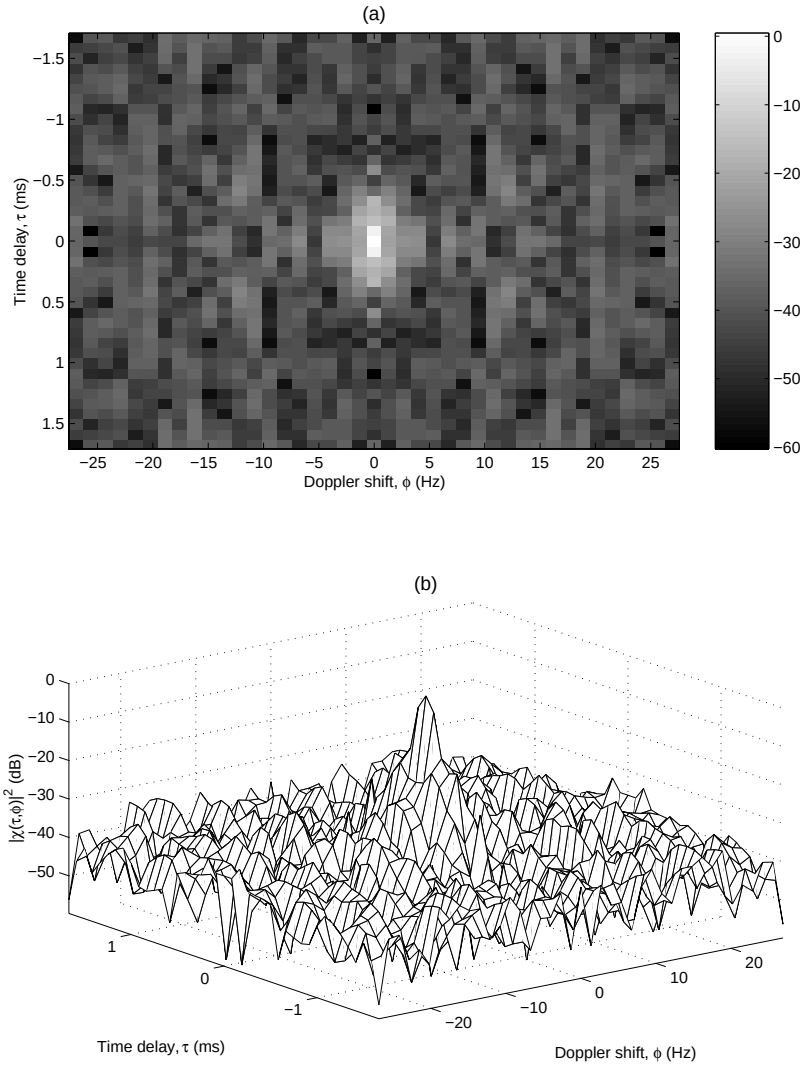

Figure 3.9: Image (a) and mesh (b) view of the ambiguity function of an example FM transmission of classical music. The example signal was 2.7 s long and supported a 12 kHz bandwidth.

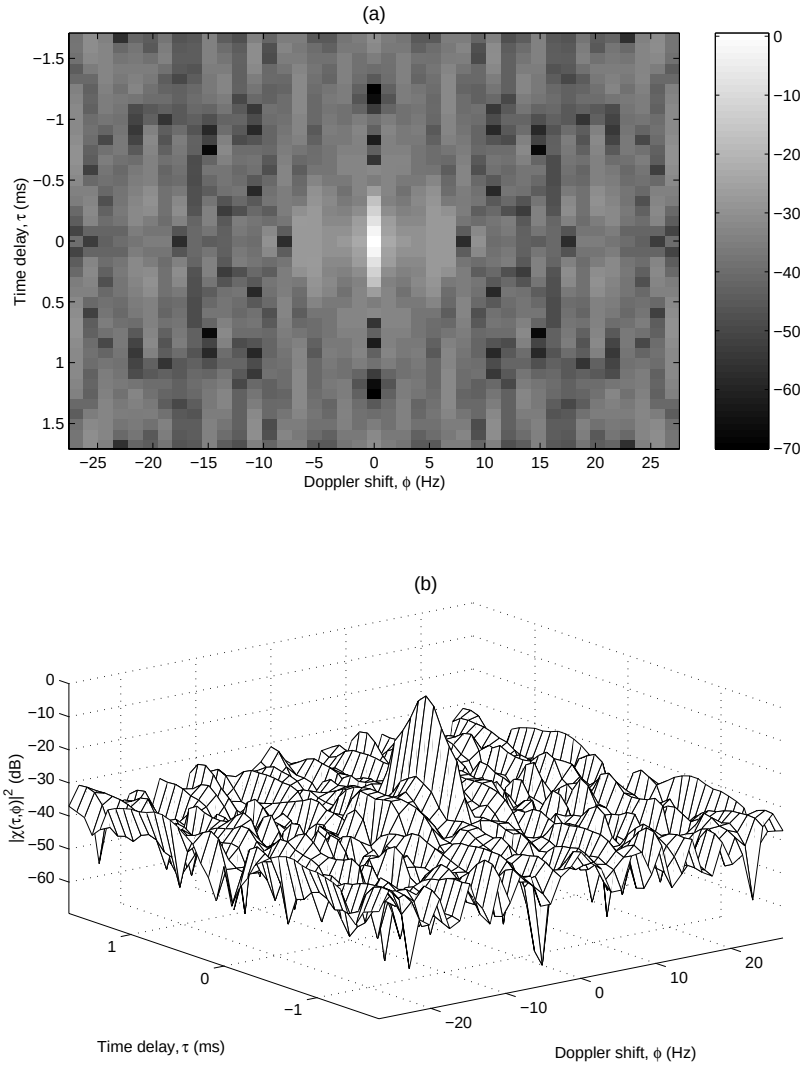

Figure 3.10: Image (a) and mesh (b) view of the ambiguity function of an example FM transmission of speech. The example signal was 2.7 s long and supported a 12 kHz bandwidth.

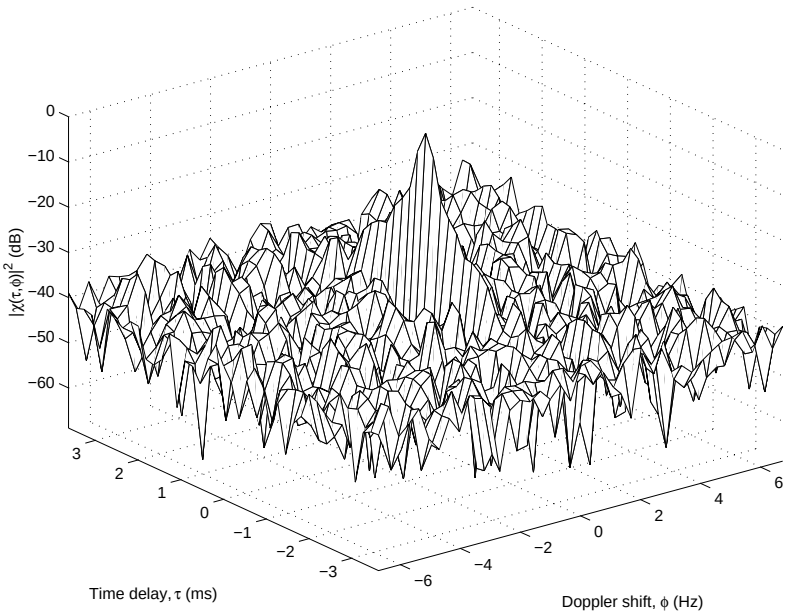

Figure 3.11: Ambiguity function from an example television broadcast. The 3 s long example signal was captured using a receiver which had 4 kHz bandwidth.

Chapter 4

Analysis of Waveforms of Opportunity

This chapter combines the radar system and particular waveforms of opportunity proposed in the previous chapter with the theory given in chapter 2. The approach taken is to calculate statistical properties of the output of the matched filter receiver, specifically the mean and variance, and determine whether it would be possible to accurately resolve the location and velocity of targets from it.

Section 4.1 states more formally the white noise model of the waveforms of opportunity, which is used throughout the remainder of the chapter. Section 4.2 applies this model to derive statistical properties of the ambiguity function, $\chi(\tau, \phi)$, of these waveforms. These results are called upon in sections 4.3 and 4.4 which calculate similar properties for the output of the matched filter and square law device, $|M(\tau, \phi)|^2$.

The mean and variance of $|M(\tau, \phi)|^2$ provide insight into the effectiveness of the transmissions of opportunity as radar waveforms. Section 4.5 discusses these results and outlines how other parameters of the radar can be modified to improve its performance.

The mean and variance of the output of the matched filter receiver also provide a method of calculating a threshold against which target detection can be performed. This is the subject of section 4.6, which completes the algorithm for converting the received signals into a list of target locations and velocities.

4.1 Model of waveforms of opportunity

As mentioned in section 3.3, the waveforms received from the proposed transmitters of opportunity are random, aperiodic and uncorrelated with themselves when delayed any more than a small amount in time or shifted any more than a small amount in frequency. An approximate model for such a signal is bandlimited Gaussian white noise.

For the analysis of this chapter, the sampled version of the waveform broadcasted from the transmitter of opportunity, $x[n]$, is modelled as a Gaussian white noise process with zero mean and variance σ_x^2. That is:

$$\mathrm{E}\{x[n]\} \quad = \quad 0 \tag{25}$$

$$\mathrm{E}\{x^2[n]\} = \sigma_x^2 \quad (26)$$

$$\mathrm{E}\{x[n]x^*[n+\tau]e^{-i\phi n}\} = 0 \text{ for } (\tau,\phi) \neq (0,0) \quad (27)$$

4.2 Analysis of the ambiguity function

It is desired to analyse $\chi(\tau,\phi)$ when the signal of interest is the transmission of opportunity, $x[n]$, as described in the previous section. From equation (10):

$$\begin{aligned} \mathrm{E}\{\chi(\tau,\phi)\} &= \frac{1}{N}\sum_{n=1}^{N}\mathrm{E}\{x[n]x^*[n+\tau]e^{-i\phi n}\} \\ &= \begin{cases} \sigma_x^2 & \text{for } (\tau,\phi)=(0,0) \\ 0 & \text{otherwise} \end{cases} \end{aligned} \quad (28)$$

where N is the number of samples in the signal. It can be further shown that:

$$\mathrm{E}\{|\chi(\tau,\phi)|^2\} = \begin{cases} (1+\frac{1}{N})\sigma_x^4 & \text{for } (\tau,\phi)=(0,0) \\ \frac{1}{N}\sigma_x^4 & \text{otherwise} \end{cases} \quad (29)$$

This equation gives an indication to the shape of the the ambiguity function of a transmission of opportunity. In order to compare this function to the predicted function of equation (17) and the example observed functions of section 3.3, this equation needs to be normalised so that $|\chi(0,0)|^2 = 1$. Normalising equation (29) provides a spike of unit height at $|\chi(0,0)|^2$ surrounded by a pedestal of value:

$$\mathrm{E}\{|\chi(\tau,\phi)|^2\} = \frac{\frac{1}{N}\sigma_x^4}{(1+\frac{1}{N})\sigma_x^4} = \frac{1}{1+N} \approx \frac{1}{N} \quad (30)$$

for large N and $(\tau,\phi) \neq (0,0)$.

Given that the received signal was sampled at the Nyquist frequency necessary to maintain the bandlimited white noise model, the time between consecutive samples is $1/B$, where B is the bandwidth of the signal. If the length of the signal is T, the number of samples is $N = TB$. Thus the height of the expected pedestal around the central spike in the ambiguity function is $1/(TB)$, confirming equation (17).

These expected values for the ambiguity function match well with the ambiguity functions of the actual transmissions of opportunity presented in section 3.3. Figure 3.5 shows a central spike surrounded by a pedestal whose average value lies around -40 dB. Given that the signal used to generate this figure had length $T = 3$ s and bandwidth $B = 4$ kHz, the height of this pedestal is expected to be $1/(TB) = 8.3 \times 10^{-5} = -40.8$ dB.

Similarly, the signal used to generate figure 3.11 was also of length $T = 3$ s and bandwidth $B = 4$ kHz, implying a constant level pedestal in the ambiguity function also of -40.8 dB, which is apparent in the figure.

Figures 3.8, 3.9 and 3.10 were each generated using signals of length $T = 2.7$ s and bandwidth $B = 12$ kHz. Thus, it is expected that these ambiguity functions contain a central spike surrounded by a pedestal of level $1/(TB) = 3.1 \times 10^{-5} = -45.1$ dB. Again, this agrees with what is seen in these images.

Up to this point, only the mean value of the ambiguity function has been considered. For further insight into the statistical properties of this random variable, it is worth calculating its variance. This also will prove valuable when considering a detection threshold for the output of the matched filter.

It can be shown that:

$$\mathrm{E}\{|\chi(\tau,\phi)|^4\} = \begin{cases} (1 + \frac{6}{N} + \frac{8}{N^2} + \frac{9}{N^3})\sigma_x^8 & \text{for } (\tau,\phi) = (0,0) \\ (\frac{3}{N^2} + \frac{6}{N^3})\sigma_x^8 & \text{otherwise} \end{cases} \tag{31}$$

So that:

$$\mathrm{VAR}\{|\chi(\tau,\phi)|^2\} = \begin{cases} (\frac{4}{N} + \frac{7}{N^2} + \frac{9}{N^3})\sigma_x^8 & \text{for } (\tau,\phi) = (0,0) \\ (\frac{2}{N^2} + \frac{6}{N^3})\sigma_x^8 & \text{otherwise} \end{cases} \tag{32}$$

The calculations used to derive these results can be found in Appendix A.3.

These equations provide first insights as to how other parameters of the radar can be modified to improve the ability to resolve targets. From equation (30) it can be seen that by increasing the number of samples in the received signal, N, the level of the pedestal in the ambiguity function decreases. This reduces the possibility that the returns from one target mask the returns from a second target with lower RCS.

These implications are discussed further in section 4.6.

4.3 Result of the matched filter (single target)

Consider the proposed passive radar configuration of section 3.1 which utilises two receivers. If there exists a single target in the region of interest the two signals received are:

$$x_o[n] = \alpha_0 x[n] + \alpha_1 x[n - t_1]e^{-iw_1 n} \tag{33}$$
$$x_r[n] = \beta_0 x[n] + \beta_1 x[n - t_1]e^{-iw_1 n} \tag{34}$$

where t_1 and w_1 are the delay in time and shift in Doppler of the transmitted signal due to the location and velocity of the target.

Note that noise is not included in the model. In the following sections it will be shown that target detection is very dependent on interference from the individual signal components of the received signals (clutter) and it is believed that the effect of noise is negligible compared with this problem.

The coefficients α_k and β_k account for the attenuation of the antenna in the direction of arrival of the two components of the received signals. As mentioned in section 3.1, the antenna linked to the receiver collecting $x_o[n]$ should be arranged so that all signals but those arriving directly from the transmitter of opportunity are attenuated, and the antenna linked to the receiver collecting $x_r[n]$ be arranged so that all signals but those arriving from the bearing being investigated for targets are attenuated.

The coefficients α_k and β_k also account for the loss and phase shift which occurs when the signal scatters from the target and the loss due to the length of the path travelled by the signal from the transmitter to the receiver.

Thus it is expected that α_0 is large, β_1 is smaller and α_1 and β_0 are close to zero. Note that due to their dependence on the location of the targets, α_k and β_k are random variables.

The result of the matched filter receiver is found by applying the above signals to equation (5):

$$
\begin{aligned}
M(\tau,\phi) &= \frac{1}{N}\sum_{n=1}^{N} x_o[n]x_r^*[n+\tau]e^{-i\phi n} \\
&= \frac{1}{N}\sum_{n=1}^{N}(\alpha_0 x[n] + \alpha_1 x[n-t_1]e^{-iw_1 n}) \\
&\quad (\beta_0 x^*[n+\tau] + \beta_1 x^*[n+\tau-t_1]e^{iw_1(n+\tau)})e^{-i\phi n} \\
&= \frac{\alpha_0\beta_0}{N}\sum_{n=1}^{N} x[n]x^*[n+\tau]e^{-i\phi n} \\
&\quad + \frac{\alpha_0\beta_1}{N}\sum_{n=1}^{N} x[n]x^*[n+\tau-t_1]e^{iw_1\tau}e^{-i(\phi+w_1)n} \\
&\quad + \frac{\alpha_1\beta_0}{N}\sum_{n=1}^{N} x[n-t_1]x^*[n+\tau]e^{-i(\phi+w_1)n} \\
&\quad + \frac{\alpha_1\beta_1}{N}\sum_{n=1}^{N} x[n-t_1]x^*[n+\tau-t_1]e^{-iw_\tau}e^{-i\phi n} \\
&= \frac{\alpha_0\beta_0}{N}\sum_{n=1}^{N} x[n]x^*[n+\tau]e^{-i\phi n} \\
&\quad + \frac{\alpha_0\beta_1}{N}e^{iw_1\tau}\sum_{n=1}^{N} x[n]x^*[n+\tau-t_1]e^{-i(\phi+w_1)n} \\
&\quad + \frac{\alpha_1\beta_0}{N}e^{-i(\phi+w_1)t_1}\sum_{n=1-t_1}^{N-t_i} x[n]x^*[n+\tau+t_1]e^{-i(\phi+w_1)n} \\
&\quad + \frac{\alpha_1\beta_0}{N}e^{-i(w_1\tau-t_1\phi)}\sum_{n=1-t_1}^{N-t_i} x[n]x^*[n+\tau]e^{-i\phi n} \\
&= a\ \chi(\tau,\phi) + b\ \chi(\tau-t_1,\phi-w_1) \\
&\quad + c\ \chi(\tau+t_1,\phi+w_1) \qquad (35)
\end{aligned}
$$

where

$$\begin{aligned} a &= \alpha_0\beta_0^* + \alpha_1\beta_1^* e^{i(w_1\tau - t_1\phi)} \\ b &= \alpha_0\beta_1^* e^{iw_1\tau} \\ c &= \alpha_1\beta_0^* e^{-i(\phi+w_1)t_1} \end{aligned}$$

This shows what was hinted to in section 2.2: that the result of the matched filter is the sum of a number of ambiguity functions, scaled and shifted according to the location and velocity of the targets. However in this case, a single target has caused three copies of the ambiguity function in the result.

The complex phases on the coefficients a, b and c are due to the different time origins of the two signals which make up the received signals. Components of the signals are delayed in time an amount t_1, yet the ambiguity function for each is calculated from the same time origin. Like the Fourier transform, a time delay in a signal causes a phase shift in the ambiguity function of that signal.

The result of squaring the matched filter output is:

$$\begin{aligned} |M(\tau,\phi)|^2 &= |a|^2|\chi(\tau,\phi)|^2 + |b|^2|\chi(\tau - t_1, \phi - w_1)|^2 \\ &\quad + |c|^2|\chi(\tau + t_1, \phi + w_1)|^2 \\ &\quad + 2\Re\{ab^*\chi(\tau,\phi)\chi^*(\tau + t_1, \phi + w_1)\} \\ &\quad + 2\Re\{ac^*\chi(\tau,\phi)\chi^*(\tau - t_1, \phi - w_1)\} \\ &\quad + 2\Re\{bc^*\chi(\tau + t_1, \phi + w_1)\chi^*(\tau - t_1, \phi - w_1)\} \end{aligned} \tag{36}$$

and

$$\begin{aligned} \mathrm{E}\{|M(\tau,\phi)|^2\} &= \mathrm{E}\{|a|^2\}\mathrm{E}\{|\chi(\tau,\phi)|^2\} \\ &\quad + \mathrm{E}\{|b|^2\}\mathrm{E}\{|\chi(\tau - t_1, \phi - w_1)|^2\} \\ &\quad + \mathrm{E}\{|c|^2\}\mathrm{E}\{|\chi(\tau + t_1, \phi + w_1)|^2\} \\ &\quad + 2\Re\{\mathrm{E}\{ab^*\}\mathrm{E}\{\chi(\tau,\phi)\chi^*(\tau + t_1, \phi + w_1)\}\} \\ &\quad + 2\Re\{\mathrm{E}\{ac^*\}\mathrm{E}\{\chi(\tau,\phi)\chi^*(\tau - t_1, \phi - w_1)\}\} \\ &\quad + 2\Re\{\mathrm{E}\{bc^*\} \\ &\quad\quad \mathrm{E}\{\chi(\tau + t_1, \phi + w_1)\chi^*(\tau - t_1, \phi - w_1)\}\} \end{aligned} \tag{37}$$

It is assumed that the phase of α_k and β_k is uniformly distributed over the interval $[0, 2\pi]$, which implies that $\mathrm{E}\{\alpha_k\} = \mathrm{E}\{\beta_k\} = 0$ for $k = 0$ or 1. Also, as the location of each of the targets is independent, both α_j and β_j are independent of both α_k and β_k for $j \neq k$.

These assumptions imply that:

$$\begin{aligned} \mathrm{E}\{ab^*\} &= \mathrm{E}\{|\alpha_0|^2\beta_0^*\beta_1 e^{-iw_1\tau} + \alpha_0^*\alpha_1|\beta_1|^2 e^{-it_1\phi}\} \\ &= \mathrm{E}\{\beta_1\}\mathrm{E}\{|\alpha_0|^2\beta_0^*\}e^{-iw_1\tau} \\ &\quad + \mathrm{E}\{\alpha_0^*\}\mathrm{E}\{\alpha_1|\beta_1|^2\}e^{-it_1\phi} \\ &= 0 \\ \mathrm{E}\{ac^*\} &= \mathrm{E}\{\alpha_0\alpha_1^*|\beta_0|^2 e^{-i(\phi+w_1)t_1} + |\alpha_1|^2\beta_0^*\beta_1 e^{-i(\tau+t_1)w_1}\} \end{aligned} \tag{38}$$

$$
\begin{aligned}
&= \mathrm{E}\{\alpha_0\}\mathrm{E}\{\alpha_1^*|\beta_0|^2\}e^{-i(\phi+w_1)t_1} \\
&\quad + \mathrm{E}\{\beta_0^*\}\mathrm{E}\{|\alpha_1|^2\beta_1\}e^{-i(\tau+t_1)w_1} \\
&= 0 \qquad (39)\\
\mathrm{E}\{bc^*\} &= \mathrm{E}\{\alpha_0\alpha_1^*\beta_0\beta_1^* e^{it_1\phi - iw_1\tau - iw_1t_1}\} \\
&= \mathrm{E}\{\alpha_0\beta_0\}\mathrm{E}\{\alpha_1^*\beta_1^*\}e^{it_1\phi - iw_1\tau - iw_1t_1} \\
&= 0 \qquad (40)
\end{aligned}
$$

and thus:

$$
\begin{aligned}
\mathrm{E}\{|M(\tau,\phi)|^2\} &= |a|^2\mathrm{E}\{|\chi(\tau,\phi)|^2\} \\
&\quad + |b|^2\mathrm{E}\{|\chi(\tau-t_1,\phi-w_1)|^2\} \\
&\quad + |c|^2\mathrm{E}\{|\chi(\tau+t_1,\phi+w_1)|^2\} \qquad (41)
\end{aligned}
$$

Incorporating information about $\mathrm{E}\{|\chi(\tau,\phi)|^2\}$, it can be seen that:

$$
\mathrm{E}\{|M(\tau,\phi)|^2\} = \begin{cases}
\left(|a|^2 + \frac{|a|^2+|b|^2+|c|^2}{N}\right)\sigma_x^4 & \text{for } (\tau,\phi) = (0,0) \\
\left(|b|^2 + \frac{|a|^2+|b|^2+|c|^2}{N}\right)\sigma_x^4 & \text{for } (\tau,\phi) = (t_1,w_1) \\
\left(|c|^2 + \frac{|a|^2+|b|^2+|c|^2}{N}\right)\sigma_x^4 & \text{for } (\tau,\phi) = (-t_1,-w_1) \\
\left(\frac{|a|^2+|b|^2+|c|^2}{N}\right)\sigma_x^2 & \text{otherwise}
\end{cases} \qquad (42)
$$

This function details the expected output of the matched filter and square-law device when a single target exists in the region of interest. The function consists of three spikes, at $(0,0)$, (t_1,w_1) and $(-t_1,-w_1)$, surrounded by a constant level pedestal.

The spikes at $(0,0)$ and $(-t_1,-w_1)$ are cross-terms due to energy from $x_o[n]$ leaking into $x_r[n]$ and visa versa, and unless suppressed, are guaranteed to produce false detections when $|M(\tau,\phi)|^2$ is compared to a detection threshold. These cross-terms are suppressed by adjusting the coefficients α_k and β_k, whose magnitudes are influenced heavily by the beam pattern of the two receivers.

Ideally, the magnitudes of α_1 and β_0 are minimised, so that the only term of significance is b. Then:

$$
\begin{aligned}
\mathrm{E}\{|M(\tau,\phi)|^2\} &= |b|^2\mathrm{E}\{|\chi(\tau-t_1,\phi-w_1)|^2\} \\
&= \begin{cases} |b|^2(1+\frac{1}{N})\sigma_x^4 & (\tau,\phi) = (t_1,w_1) \\ |b|^2\frac{1}{N}\sigma_x^4 & \text{otherwise} \end{cases} \\
&= \begin{cases} |\alpha_0|^2|\beta_1|^2(1+\frac{1}{N})\sigma_x^4 & (\tau,\phi) = (t_1,w_1) \\ |\alpha_0|^2|\beta_1|^2\frac{1}{N}\sigma_x^4 & \text{otherwise} \end{cases} \qquad (43)
\end{aligned}
$$

Note that this expression is the same as that for $\mathrm{E}\{|\chi(\tau,\phi)|^2\}$, only shifted over (t_1,w_1) and scaled by $|\alpha_0|^2|\beta_1|^2$. Thus if the output of the matched filter is normalised so that

the maximum value is unity, the result is expected to be a spike of unit height at (t_1, w_1) surrounded by a constant level pedestal of value:

$$\mathrm{E}\{|M(\tau,\phi)|^2\} = \frac{|\alpha_0|^2|\beta_1|^2(1+1/N)\sigma_x^4}{|\alpha_0|^2|\beta_1|^2(1/N)\sigma_x^4} \approx \frac{1}{N} \tag{44}$$

for large N and $(\tau,\phi) \neq (t_1, w_1)$.

If the single receiver radar configuration of section 3.1.2 is used, the two input signals to the matched filter are the same and $\alpha_k = \beta_k$. In this case, it would be impossible to minimise the cross-terms and the ability to detect the target would depend on the ability to determine which of the three peaks of the matched filter corresponded to it.

If the received signal was scaled such that $|\alpha_1| = 1$, the result of the matched filter when a single receiver is used is:

$$\begin{aligned}\mathrm{E}\{|M(\tau,\phi)|^2\} &= (1+|\alpha_0|^4)\mathrm{E}\{|\chi(\tau,\phi)|^2\} \\ &\quad + |\alpha_0|^2\mathrm{E}\{|\chi(\tau-t_1,\phi-w_1)|^2\} \\ &\quad + |\alpha_0|^2\mathrm{E}\{|\chi(\tau+t_1,\phi+w_1)|^2\}\end{aligned} \tag{45}$$

It is desired that the peak at (t_1, w_1) is maximised compared to the peak at the origin, as there is concern that the former peak may be masked by the pedestal of the ambiguity function centred at the origin. That is, the value of $|\alpha_0|$ is sought which maximises:

$$\frac{|\alpha_0|^2}{(1+|\alpha_0|^4)} \tag{46}$$

The required value of $|\alpha_0|$ is 1. Thus, when a single receiver is used, it is desired to fix the attenuation of the antenna in the direction of the transmitter so that the received signal scattered from the target is equally as powerful as the direct signal.

Note that substituting $|\alpha_0| = 1$ into the previous equation produces 1/2, thus when a single receiver is used, the maximum height of the peak corresponding to the target is 3 dB less than the peak at the origin.

These calculations define the expected value of the matched filter output. An approximation of the variance of this function is:

$$\begin{aligned}\mathrm{VAR}\{|M(\tau,\phi)|^2\} &= |a|^2\ \mathrm{VAR}\{|\chi(\tau,\phi)|^2\} \\ &\quad + |b|^2\ \mathrm{VAR}\{|\chi(\tau-t_1,\phi-w_1)|^2\} \\ &\quad + |c|^2\ \mathrm{VAR}\{|\chi(\tau+t_1,\phi+w_1)|^2\}\end{aligned} \tag{47}$$

where $\mathrm{VAR}\{|\chi(\tau,\phi)|^2\}$ is given in equation (32).

When the magnitudes of α_1 and β_0 are minimised and b is the only term of significance, this expression simplifies to:

$$\mathrm{VAR}\{|M(\tau,\phi)|^2\} = \begin{cases} |\alpha_0|^2|\beta_1|^2(\frac{4}{N}+\frac{7}{N^2}+\frac{9}{N^3})\sigma_x^8 & \text{for } (\tau,\phi)=(t_1,w_1) \\ |\alpha_0|^2|\beta_1|^2(\frac{2}{N^2}+\frac{6}{N^3})\sigma_x^8 & \text{otherwise} \end{cases} \tag{48}$$

Section 4.6 describes how these results can be used to determine the necessary threshold that should be applied to $|M(\tau,\phi)|^2$ in order to detect targets.

4.4 Result of the matched filter (general case)

If there are K targets in the region of interest, equations (33) and (34) can be extended to be:

$$x_o[n] = \sum_{k=0}^{K} \alpha_k x[n-t_k] e^{-iw_k n} \tag{49}$$

$$x_r[n] = \sum_{k=0}^{K} \beta_k x[n-t_k] e^{-iw_k n} \tag{50}$$

where t_k and w_k indicate the amount of time delay and frequency shift produced by the location and velocity of the k-th target. As the signal arriving directly from the transmitter of opportunity usually undergoes no delay in time or shift in Doppler (or at least all other time delays and Doppler shifts are normalised to this signal), it is expected that $t_k = w_k = 0$ for one component of these two signals (say, the one for $k = 0$).

As in the previous section, the coefficients α_k and β_k refer to the attenuation of the component of the signal reflected from the k-th target.

Applying equation (5) to the scenario described above, the result of the matched filter is:

$$\begin{aligned}
M(\tau,\phi) &= \frac{1}{N}\sum_{n=1}^{N} x_o[n] x_r^*[n+\tau] e^{-i\phi n} \\
&= \frac{1}{N}\sum_{n=1}^{N}\sum_{j=0}^{K}\sum_{k=0}^{K} \alpha_j\beta_k x[n-t_j] e^{-iw_j n} \\
&\quad x^*[n+\tau-t_k] e^{iw_k(n+\tau)} e^{-i\phi n} \\
&= \frac{1}{N}\sum_{j=0}^{K}\sum_{k=0}^{K}\sum_{n=1-t_j}^{N-t_j} \alpha_j\beta_k x[n] x^*[n+t_j-t_k+\tau] \\
&\quad e^{-i(w_j n + w_j t_j - w_k n - w_k t_j - w_j\tau + \phi n + \phi t_j)} \\
&= \frac{1}{N}\sum_{j=0}^{K}\sum_{k=0}^{K} \alpha_j\beta_k e^{-i((\phi+w_j-w_k)t_j - w_k\tau)} \\
&\quad \sum_{n=1-t_j}^{N-t_j} x[n] x^*[n+(\tau+t_j-t_k)] e^{-i(\phi+w_j-w_k)} \\
&= \frac{1}{N}\sum_{j=0}^{K}\sum_{k=0}^{K} \gamma_{j,k}\, \chi(\tau+t_j-t_k, \phi+w_j-w_k)
\end{aligned} \tag{51}$$

where $\gamma_{j,k} = \alpha_j\beta_k e^{-i((\phi+w_j-w_k)t_j - w_k\tau)}$.

The result of squaring the matched filter output is:

$$\begin{aligned}
|M(\tau,\phi)|^2 &= \frac{1}{N^2}\sum_{k_1=0}^{K}\sum_{k_2=0}^{K}\sum_{k_3=0}^{K}\sum_{k_4=0}^{K} \gamma_{k_1,k_2}\, \gamma_{k_3,k_4}^* \\
&\quad \chi(\tau+t_{k_1}-t_{k_2}, \phi+w_{k_1}-w_{k_2}) \\
&\quad \chi^*(\tau+t_{k_3}-t_{k_4}, \phi+w_{k_3}-w_{k_4})
\end{aligned} \tag{52}$$

and

$$\begin{aligned}\mathrm{E}\{|M(\tau,\phi)|^2\} &= \frac{1}{N^2}\sum_{k_1=0}^{K}\sum_{k_2=0}^{K}\sum_{k_3=0}^{K}\sum_{k_4=0}^{K}\mathrm{E}\{\gamma_{k_1,k_2}\,\gamma^*_{k_3,k_4}\}\\ &\quad \mathrm{E}\{\chi(\tau+t_{k_1}-t_{k_2},\phi+w_{k_1}-w_{k_2})\\ &\quad \chi^*(\tau+t_{k_3}-t_{k_4},\phi+w_{k_3}-w_{k_4})\} \qquad (53)\end{aligned}$$

where

$$\begin{aligned}\mathrm{E}\{\gamma_{k_1,k_2}\gamma^*_{k_3,k_4}\} &= \mathrm{E}\{\alpha_{k_1}\beta_{k_2}\alpha^*_{k_3}\beta^*_{k_4}\}\\ &\quad e^{-i((\phi+w_{k_1}-w_{k_2})t_{k_1}-(\phi+w_{k_3}-w_{k_4})t_{k_3}-(w_{k_2}-w_{k_4})\tau)}\end{aligned}$$

Again it is assumed that $\mathrm{E}\{\alpha_k\}=\mathrm{E}\{\beta_k\}=0$ and that both α_j and β_j are independent of both α_k and β_k for $j\neq k$.

These assumptions imply that:

$$\begin{aligned}\mathrm{E}\{\gamma_{k_1,k_2}\gamma^*_{k_3,k_4}\} &= \delta_{k_1-k_3}\delta_{k_2-k_4}\mathrm{E}\{\alpha_{k_1}\beta_{k_2}\alpha^*_{k_3}\beta^*_{k_4}\}\\ &\quad e^{-i((\phi+w_{k_1}-w_{k_2})t_{k_1}-(\phi+w_{k_3}-w_{k_4})t_{k_3})} \qquad (54)\end{aligned}$$

where δ_j is 1 for $j=0$ and 0 otherwise.

Equation (53) can thus be written as:

$$\begin{aligned}\mathrm{E}\{|M(\tau,\phi)|^2\} &= \frac{1}{N^2}\sum_{j=0}^{K}\sum_{k=0}^{K}\mathrm{E}\{|\gamma_{j,k}|^2\}\\ &\quad \mathrm{E}\{|\chi(\tau+t_j-t_k,\phi+w_j-w_k)|^2\}\\ &= \frac{1}{N^2}\sum_{j=0}^{K}\sum_{k=0}^{K}\mathrm{E}\{|\alpha_j|^2|\beta_k|^2\}\\ &\quad \mathrm{E}\{|\chi(\tau+t_j-t_k,\phi+w_j-w_k)|^2\} \qquad (55)\end{aligned}$$

This equation shows that the square of the matched filter is the sum of up to $(K+1)^2$ copies of the ambiguity function, which appear as $(K+1)^2$ peaks across the (τ,ϕ) plane. Of these, only K correspond to actual targets and the remainder are the undesired cross-terms.

As for the single target case, these cross-terms are reduced by adjusting the magnitudes of α_k and β_k. Note that effective reduction in these cross-terms is possible by manipulating only one of these sets of coefficients. For example, if the receiver collecting the direct signal substantially rejects signals from any other direction, $|\alpha_k|$ will be approximately zero for all k but one. If it is $|\alpha_0|$ that is non-zero, and the direct signal is indeed direct (that is, $t_0=w_0=0$), then equation (53) becomes:

$$\begin{aligned}\mathrm{E}\{|M(\tau,\phi)|^2\} &= \frac{1}{N^2}\sum_{k=0}^{K}\mathrm{E}\{|\alpha_0|^2|\beta_k|^2\}\\ &\quad \mathrm{E}\{|\chi(\tau-t_k,\phi-w_k)|^2\} \qquad (56)\end{aligned}$$

which corresponds to a peak at the origin and K other peaks, each located at a time delay, t_k, and Doppler shift, w_k, corresponding to the k-th target.

In the configuration using a single antenna, $\alpha_k = \beta_k$ and $x_o[n] = x_r[n]$. In this case equation (53) becomes:

$$\begin{aligned} \mathrm{E}\{|M(\tau,\phi)|^2\} &= \frac{1}{N^2}\sum_{j=0}^{K}\sum_{k=0}^{K}\mathrm{E}\{|\alpha_j|^2|\alpha_k|^2\} \\ &\quad \mathrm{E}\{|\chi(\tau+t_j-t_k,\phi+w_j-w_k)|^2\} \end{aligned} \tag{57}$$

Thus for the single receiver configuration, it is much more difficult to reduce the cross-terms in the matched filter output.

4.5 Resolution issues re-visited

Section 2.3 provided a general discussion on how the shape of the radar waveform, and more specifically the shape of its ambiguity function, can affect the ability of the radar to resolve target location and velocity. This section examines the results of the previous three sections to draw more specific conclusions on the performance of the proposed radar system and waveforms of opportunity.

It is evident that the output of the matched filter is the combination of a number of ambiguity functions, each shifted to the time delay and Doppler shift corresponding to a target (or false target in the case of cross-terms), and scaled by some amount. Each ambiguity function consists of a peak at the origin surrounded by a constant level pedestal. This result suggests two possible problems:

- That the peaks due to cross-terms produce false target detections, and
- That a copy of the ambiguity function due to one target is scaled such that the constant level pedestal away from its origin is larger than the peak of the ambiguity function due to another target, rendering the second target undetectable.

As mentioned already, the solution to the first problem is to adjust the antenna gain pattern. Note that there need not be perfect attenuation of signals arriving from directions other that the direction of interest for the cross-terms to be avoided. For example, if there exists two targets and the powers in the received signals are normalised so that the direct wave has a power of unity, the scattered signals will typically contain power much less than unity, that is, $|\alpha_0|$ in equation (49) is 1 and $|\beta_1|$ and $|\beta_2|$ in equation (50) are less than 1. The peaks in the matched filter output corresponding to the two targets will have height $|\beta_1|^2$ and $|\beta_2|^2$ while the cross-terms will have height $|\beta_1|^2 \times |\beta_2|^2$, which is far less.

Although cross-terms produced by the interaction of returns from multiple targets are often negligible, the interaction between the amount of the direct signal in both $x_r[n]$ and $x_o[n]$ usually produces a peak in the origin of the matched filter output of significant magnitude. This cross-term is usually the cause of the second problem of the two listed above.

The power of the direct signal is:

$$P_o = \frac{P_t \lambda^2}{(4\pi)^2 r_0^2} \tag{58}$$

where P_t is the power used by the transmitter, λ is the wavelength of the carrier frequency and r_0 is the distance from the transmitter to the receiver. The power of a signal scattered from a target and received at the radar is:

$$P_r = \frac{P_t \lambda^2 \sigma}{(4\pi)^3 (r_1 r_2)^2} \tag{59}$$

where r_1 is the distance from the transmitter to the target and r_2 is the distance from the target to the receiver.

Typically, P_r is significantly less than P_o so even with substantial attenuation of the direct signal, the coefficient $|\beta_0|$ in equation (34) is significant and the matched filter output contains the peak at the origin that was mentioned earlier.

The ratio of the power of the two received signals is:

$$\frac{P_r}{P_o} = \frac{1}{4\pi} \frac{\sigma r_0^2}{(r_1 r_2)^2} \tag{60}$$

This value is the difference in height of the two peaks in the matched filter output that occur if the antenna at the receiver was omni-direction. If this value is more negative than the level of the pedestal of the ambiguity function centred at the origin, the target is lost. Attenuation towards the transmitter reduces P_o and increases the height of the peak due to the target compared to the peak at the origin. The amount of attenuation required is the amount which brings the height of the peak due to the target above the pedestal around the peak at the origin.

The constant level pedestal surrounding the various peaks in the matched filter output is often called the clutter.

4.6 Target detection

As mentioned in section 2.1, optimally detecting targets involves comparing the output of the matched filter, $|M(\tau, \phi)|^2$, against a single threshold and determining at which values of τ and ϕ the threshold is exceeded. An obvious question is what to set the threshold to.

The previous sections of this chapter showed that the output of the matched filter and square-law device is a number of peaks corresponding to the returns from targets surrounded by a constant level pedestal. Thus the detection threshold is required to separate the peaks from the pedestal.

Detection theory provides a number of methods for which to optimally determine this threshold, however the choices are drastically reduced for the radar problem as the likelihood of a target being present at a given time delay or Doppler shift cannot be known. One method which is often used is the Neyman-Pearson detector [27].

The Neyman-Pearson detector involves calculating the detection threshold so that the probability of falsely determining the presence of a target is fixed. For the receiver output described above this involves calculating the threshold so that a fixed number of (τ, ϕ) pairs which occur in the pedestal produce values of $|M(\tau, \phi)|^2$ which exceed the threshold.

This calculation requires the probabilistic distribution of the values of the output of the matched filter receiver which lie in the constant level pedestal. This could be estimated by sampling the matched filter output at values of τ and ϕ which are known not to contain any peaks due to targets.

Alternatively, the distribution could be assumed to be a particular type, such as Gaussian or chi-squared, which is totally described by the two moments (mean and variance) calculated in the previous sections. For example, if the distribution is assumed Gaussian and the probability of false alarm is set to 1 in 100, the detection threshold would be 3 standard deviations above the mean. If there existed a single target in the region of interest and the antennas were such that the amount of direct signal contributing to $x_r[n]$ and the amount of scattered signal contributing to $x_o[t]$ was negligible, the mean of the output of the matched filter receiver is given in equation (43) and its variance in equation (48). If the output is normalised so that the peak at (t_1, w_1) is unity, the necessary detection threshold would be:

$$l = \frac{1}{N} + 3\left(\frac{2}{N^2} + \frac{6}{N^3}\right) \tag{61}$$

Often this detection step is not the final processing performed on the received signals. Tracking and the algorithms mentioned in section 3.2 which consider how target detections vary with time are also used to minimise false detections. For this reason, the probability of false detection used when calculating the above threshold is often fixed to be slightly more than what is ultimately desired.

Chapter 5

Simulations and Examples

The previous chapters provide insight as to how it may be possible to use transmissions such as radio and television broadcasts as the waveform for passive radar. This chapter provides a number of simulations of this concept and discussions on how the ideas presented in this report could be used.

These simulations provide some confirmation of the results attained in chapter 4 and an initial picture of the performance of the suggested passive radar.

5.1 FM radio

One possibility for the proposed passive radar is to inconspicuously monitor ships and aircraft arriving at and departing from a particular city or location of interest. The example city chosen for the first simulation was Darwin, the largest port along Australia's northern coast and the transmitter of opportunity was a local FM radio station located on the city's edge.

The receiver was located 62 km away. It is worth noting again that the radar emits no signal energy and could therefore be hidden.

This simulation examines the ability to detect a single ship which is approaching Darwin. An illustration of the scenario is shown in figure 5.1 and the parameters of simulation are listed in the following table:

Simulated scenario:	
Distance from Transmitter to Receiver (r_0)	62.0 km
Distance from Transmitter to Target (r_1)	21.4 km
Distance from Target to Receiver (r_2)	73.5 km
Target velocity (v)	48 km/hr
Target RCS (σ)	250 m^2
Transmitter carrier frequency (f_c)	103.3 MHz
Receiver characteristics:	
Attenuation directly towards the transmitter (β_0)	-50 dB
Radar integration time (T)	2.8 s
Receiver bandwidth (B)	4 kHz

It is assumed that a linear array of antennas was being used to collect the incoming waveforms. In theory such arrays are capable of totally rejecting signals arriving from a particular direction however in practice the depth of any null is governed by how well the array is calibrated. As emphasised already in earlier chapters, the ability to attenuate the direct signal is very important to the performance of the radar.

As with all the simulations in this chapter, the received signals were considered digital, having been sampled upon being received. Thus, the result of the matched filter was evaluated at intervals of $1/B$ along the τ axis and $1/T$ along the ϕ axis (this process is explained further in section 2.5). This implies the length of a resulting range-Doppler cell was $c/4000 = 75$ km along the axis corresponding to total range and $c/(Tf_c) = 3.73$ km/hr along the axis corresponding to velocity. Thus the parameters of the radar defined here have the potential to provide satisfactory resolution in target velocity but not in range for the given scenario. This is illustrated in figure 5.1 which shows ellipses marking the edge of the first and second range cells.

The ambiguity function of the waveform of opportunity which was used in this simulation is shown in figure 5.2. This waveform was an actual recording from an FM radio transmission.

The radar waveform was delayed in time and shifted in Doppler the appropriate amount to simulate the location and velocity of the target. This signal and the original waveform were both scaled to simulate the path loss due to distance travelled and combined to form the two received signals $x_o[n]$ and $x_r[n]$. These signals became the input to the matched

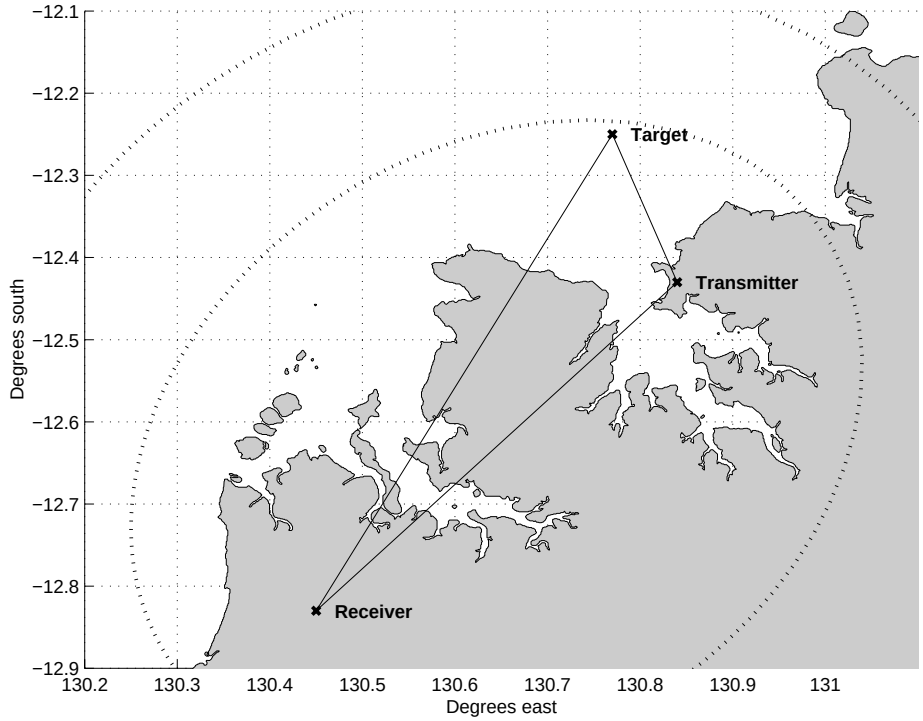

Figure 5.1: First proposed simulation. The dotted ellipses mark the extent of the first and second range cells.

filter, as dictated in equation (5). The output of this filter and the result of this first simulation is shown in figure 5.3.

In this figure the peak due to the target can be just seen above the clutter floor caused by the direct signal and the copy of the ambiguity function located at the origin. The level of this clutter floor is expected to be $1/(TB) = 8.93 \times 10^{-5} = -40.5$ dB and the ratio of power in the scattered signal to that in the direct signal is:

$$\begin{aligned} \frac{P_r}{P_o} &= \frac{1}{4\pi} \frac{250 \times 62000^2}{(21400 \times 73500)^2} \\ &= 3.09 \times 10^{-8} \\ &= -75.1 \text{ dB} \end{aligned}$$

From this it can be seen that without the attenuation of the array in the direction of the transmitter, the power in the scattered signal would be dominated by the clutter floor. With the attenuation in place however, the difference between the powers becomes $-75.1 + 50 = -25.1$ dB, pushing the height of the peak due to the target above the clutter floor. These results can be seen in figure 5.3.

Using equation (48) and the fact that the matched filter output has been normalised, the variance of the clutter floor is:

$$\frac{2}{(2.8 \times 4000)^2} + \frac{6}{(2.8 \times 4000)^3} = 2.23 \times 10^{-8}$$

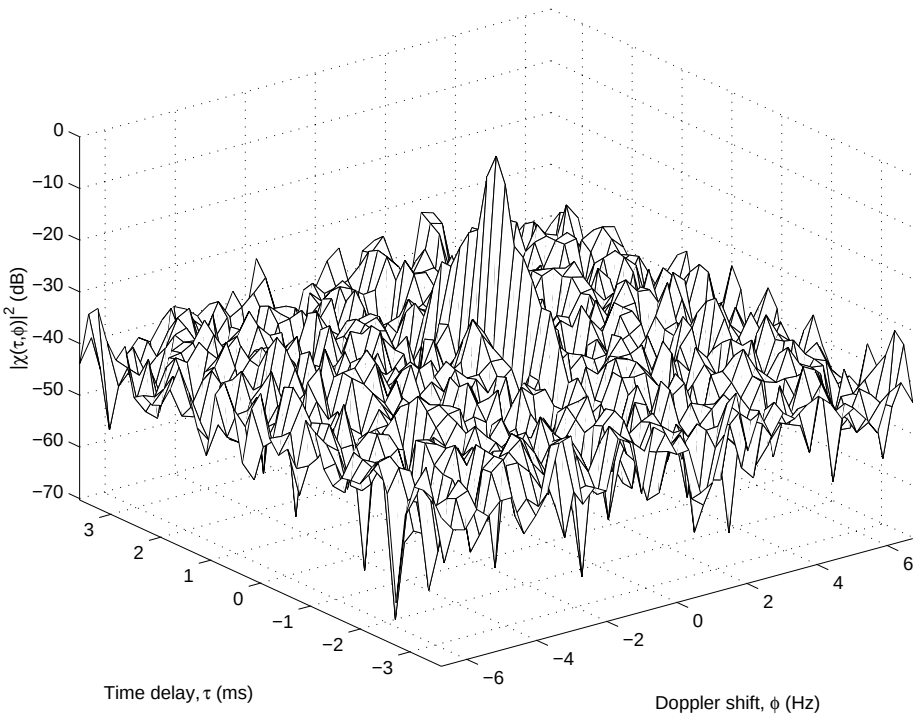

Figure 5.2: Ambiguity function of the waveform of opportunity for the first simulation. The waveform had length $T = 2.8$ s and bandwidth $B = 4$ kHz.

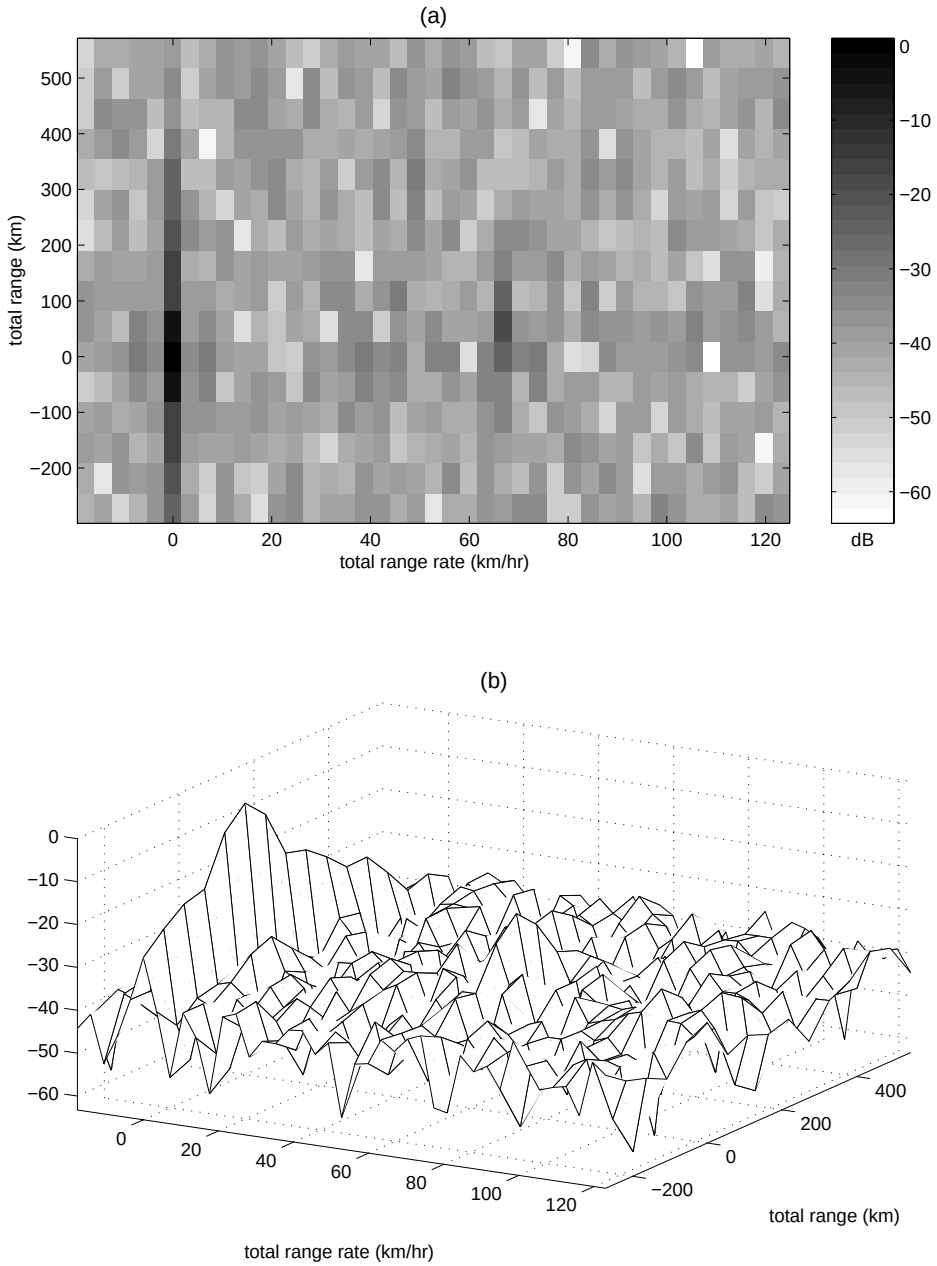

Figure 5.3: Result of the matched filter for the first simulation.

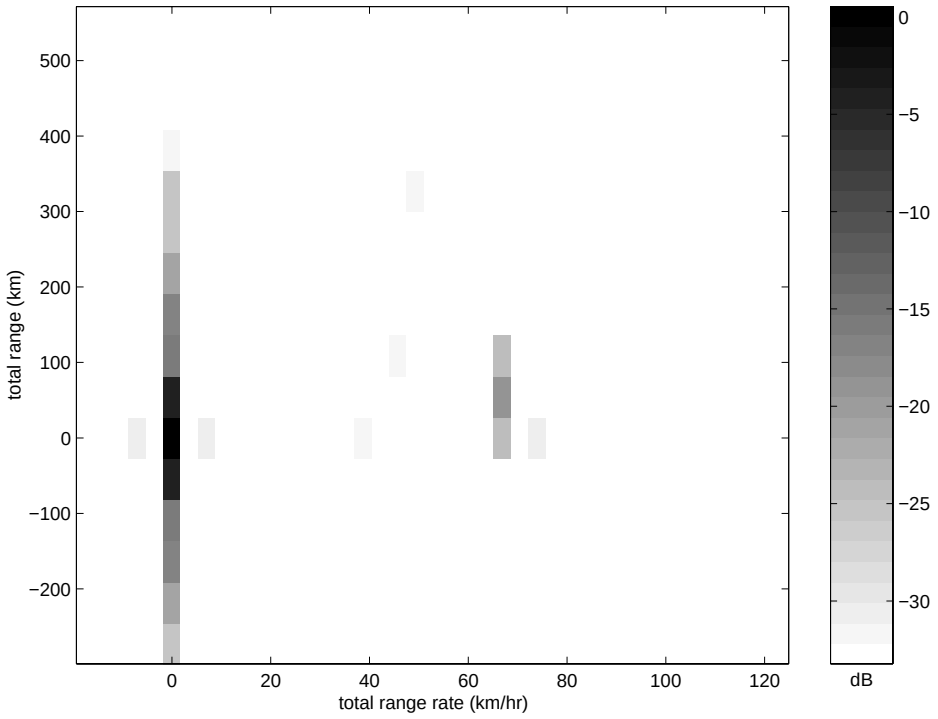

Figure 5.4: Result of the matched filter after thresholding at 3 standard deviations above the expected clutter floor (first simulation).

Thus, three standard deviations above the clutter floor comes to -32.7 dB. Thresholding the output of the matched filter at this value is illustrated in figure 5.4.

This figure clearly shows both the peak due to the direct signal and the peak due to the target. Also apparent in this figure are six range-Doppler cells where the matched filter output exceeded the threshold at values of τ and ϕ for which there was no target. The figure contains 640 range-Doppler cells corresponding to the clutter floor, so the probability of false alarm appears to be $6/640 = 0.009$, close to the expected 1 percent.

From these results it seems the suggested configuration was able to successfully detect the target and calculate its total range and rate of change of total range[4] although range resolution was particularly poor. In an effort to improve upon range resolution, the previous simulation was executed a second time using a signal of bandwidth $B = 48$ kHz.

In this second simulation, all parameters remained the same except the bandwidth of the receivers. The length of a range-Doppler cell along the range axis for this simulation is $c/B = 6.25$ km, thus it is expected to be able to resolve the location of targets on a much finer grid. This is illustrated in figure 5.5.

The ambiguity function of the waveform used in this second simulation is shown in figure 5.6. It should be noted that this signal was simulated by frequency modulating a sample of music as a receiver with a bandwidth of up to 48 kHz was unavailable during the course of preparing this report. Nevertheless, the ambiguity function appears typical of

[4]Conversion from total range and rate of change of total range to target location and velocity is provided in section 3.2.

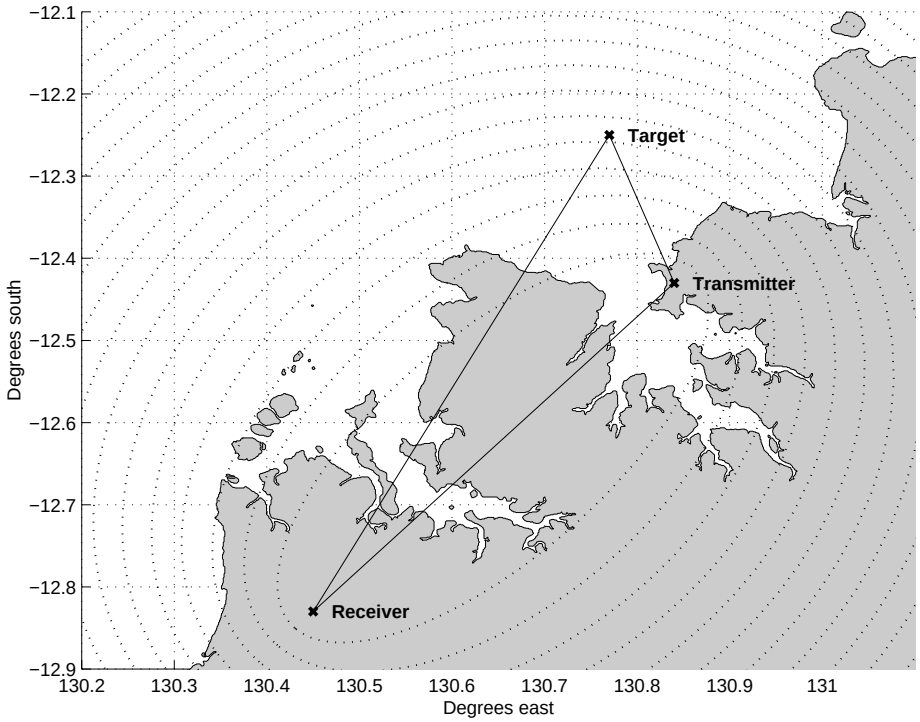

Figure 5.5: Second proposed simulation. The dotted ellipses mark the extent of the ranges cells.

that generated from a transmission of opportunity and contains the expected constant level pedestal of $1/(TB) = -51.3$ dB (more than 10 dB lower than the pedestal of figure 5.1).

The result of the matched filter can be seen in figure 5.7. As the location of the target and amount of attenuation of the receiver towards the transmitter has not changed, the difference of heights of the two peaks in $|M(\tau, \phi)|^2$ is still -25.1 dB. The increase in bandwidth however, has caused the clutter floor around the peaks to drop 10.8 dB. This implies that the attenuation of the receivers in the direction of the direct signal could have been 10.8 dB worse and the target would still have been as visible as it was in the first simulation.

This figure also shows that the location of the target causes a peak in the fifth range cell, as opposed to the first, which was the case in the first simulation. Thus it is possible to resolve to better accuracy the location of the target.

For this second simulation, three standard deviations above the clutter floor corresponds to -44.1 dB. The result of the matched filter thresholded at this value is shown in figure 5.8. As can be seen from this figure, the peak corresponding to the target sits strong above the threshold, however there appears to be a much greater amount of the $|M(\tau, \phi)|^2$ surface which also sits above it. Much of these detections are due to the wide peak at the origin. The transmissions of opportunity are not exactly white noise and the peak at the origin of their ambiguity function has finite width.

One final note on the benefits of increasing receiver bandwidth is shown in figure 5.9. Part (a) of this figure shows, for each location on the map, the amount of energy arriving

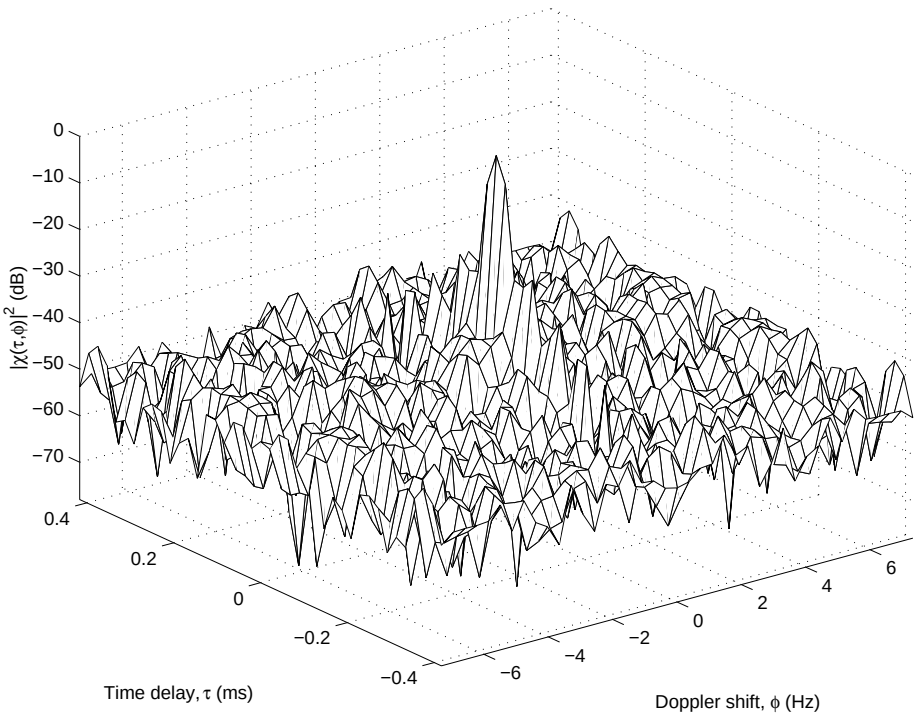

Figure 5.6: Ambiguity function of the waveform of opportunity for the second simulation. The waveform had length $T = 2.8$ s and bandwidth $B = 48$ kHz.

at the receiver due to the scattering off a target at that location. Part (b) shows the same information as part (a), but only for those locations which produce signals of energy $-44.1 - 50 = -94.1$ dB and $-32.7 - 50 = -82.7$ dB. That is, the two ellipses of part (b) mark the edge of detection for the receivers of the two simulations (the inside ellipse corresponds to the detection threshold used in the first simulation). Any target located beyond an ellipse produces a scattered signal whose energy would not be enough for the peak in the matched filter output to appear above the given detection threshold.

As can be seen from this figure, the receiver using the higher bandwidth can detect targets at a much further range.

5.2 Television broadcasts

The previous section showed that by increasing the bandwidth of the receiver to 48 kHz, the radar was able to resolve the location of the target to within approximately 6 km. In order to resolve targets to a finer resolution, the required bandwidth is greater. Of the three types of transmissions of opportunity investigated in this report, the only ones which contain energy distributed across such large bandwidths are television broadcasts.

As mentioned in section 3.3, television broadcasts support a bandwidth of 6 MHz. If the bandwidth of the receiver was half of this, the location of targets could be determined to within $c/(3 \times 10^6) = 100$ m. Television broadcasts however, contain a dominant pulse occurring every 64 μs which produce ridges 64 μs apart in the ambiguity function and

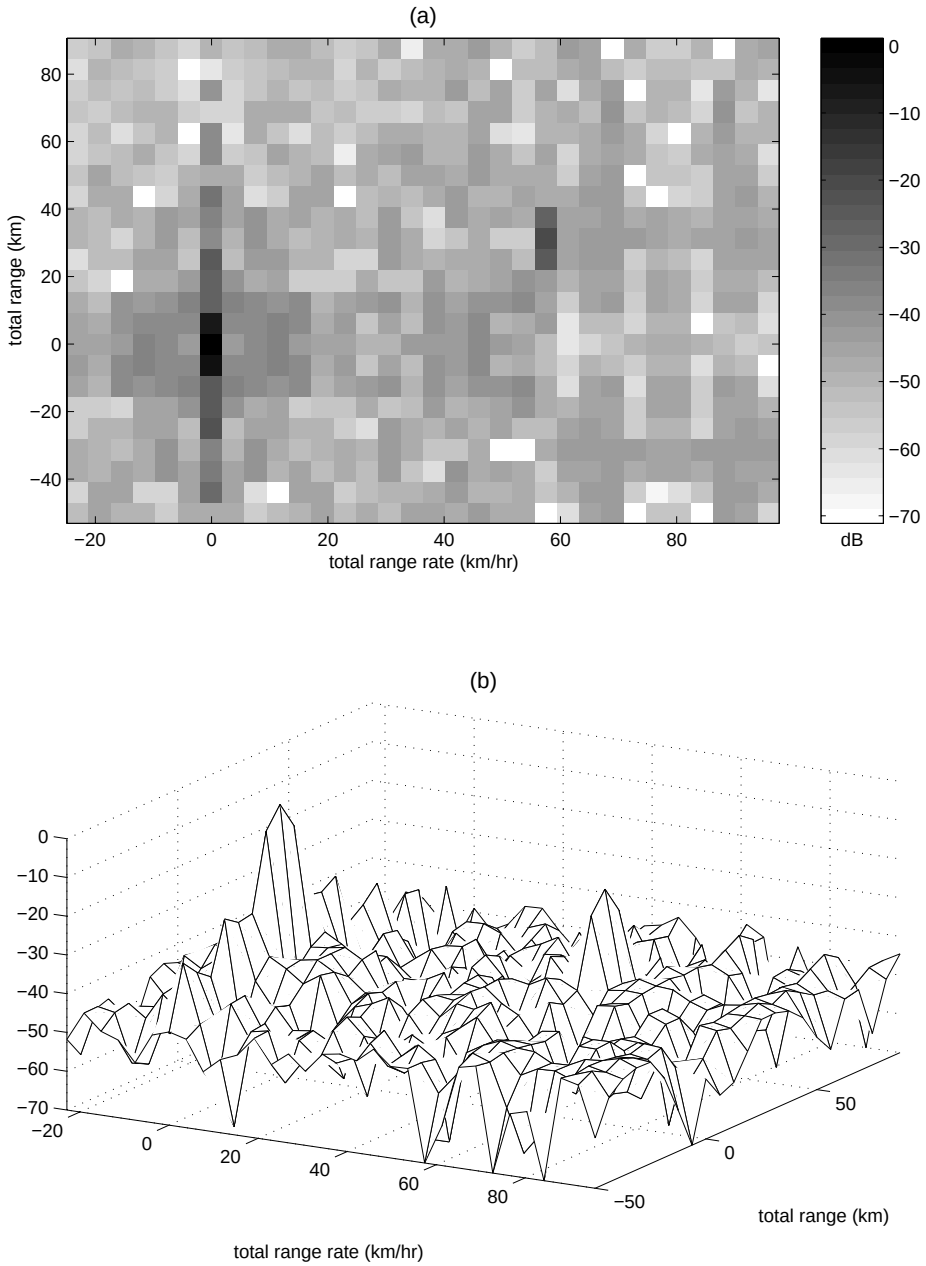

Figure 5.7: Result of the matched filter for the second simulation.

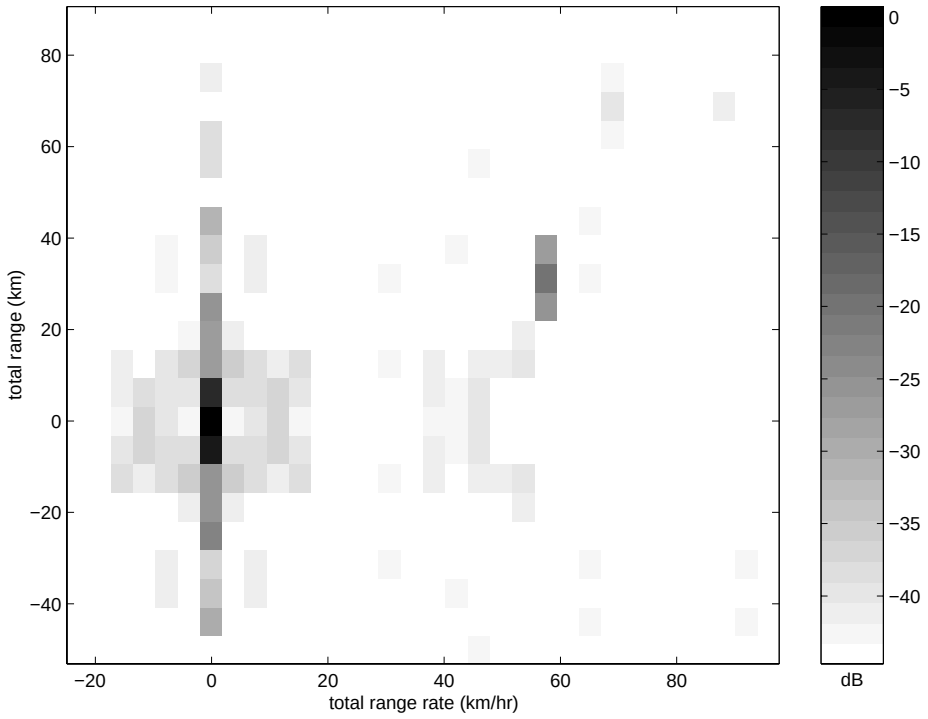

Figure 5.8: Result of the matched filter after thresholding at 3 standard deviations above the expected clutter floor (second simulation).

multiple peaks in the matched filter output when a single target is present in the region of interest.

A time delay of 64 μs corresponds to a total range of $c \times 64 \times 10^{-6} = 19.2$ km. Thus a target whose total range was $19.2 + d$ km could be mistaken for a target whose total range was only d km. One solution to this ambiguity is to scan only for targets of total range less than $19.2 + r_0$ km and to select a time-bandwidth product such that the returns from targets beyond this range fall below the detection threshold.

The scenario chosen for the simulation utilising television broadcasts consists of the receiver located $r_2 = 2$ km from an airport of interest and $r_0 = 50$ km from a television broadcast tower. The relative locations of the receiver, transmitter and airport is shown in figure 5.10. Also shown on this figure is, for each (x, y) location, the amount of energy arriving at the receiver due to the scattering off a target at that location, and an ellipse corresponding to a total bistatic range of $50 + 19.2 = 69.2$ km. The RCS of the target was assumed to be 150 m^2.

In order to minimise the detection of targets beyond the ambiguous range, the receiver need only be accurate enough to detect scattered signals with power greater than approximately -70 dB lower than that from the direct signal. This allows the receiver to scan for targets to, at best, approximately 10 km away from the airport.

If the receiver antenna provided 20 dB of attenuation towards the transmitter, the required detection threshold would be about -50 dB. Given that the receiver uses a bandwidth of 3 MHz, the signal duration required to move the clutter floor below this threshold

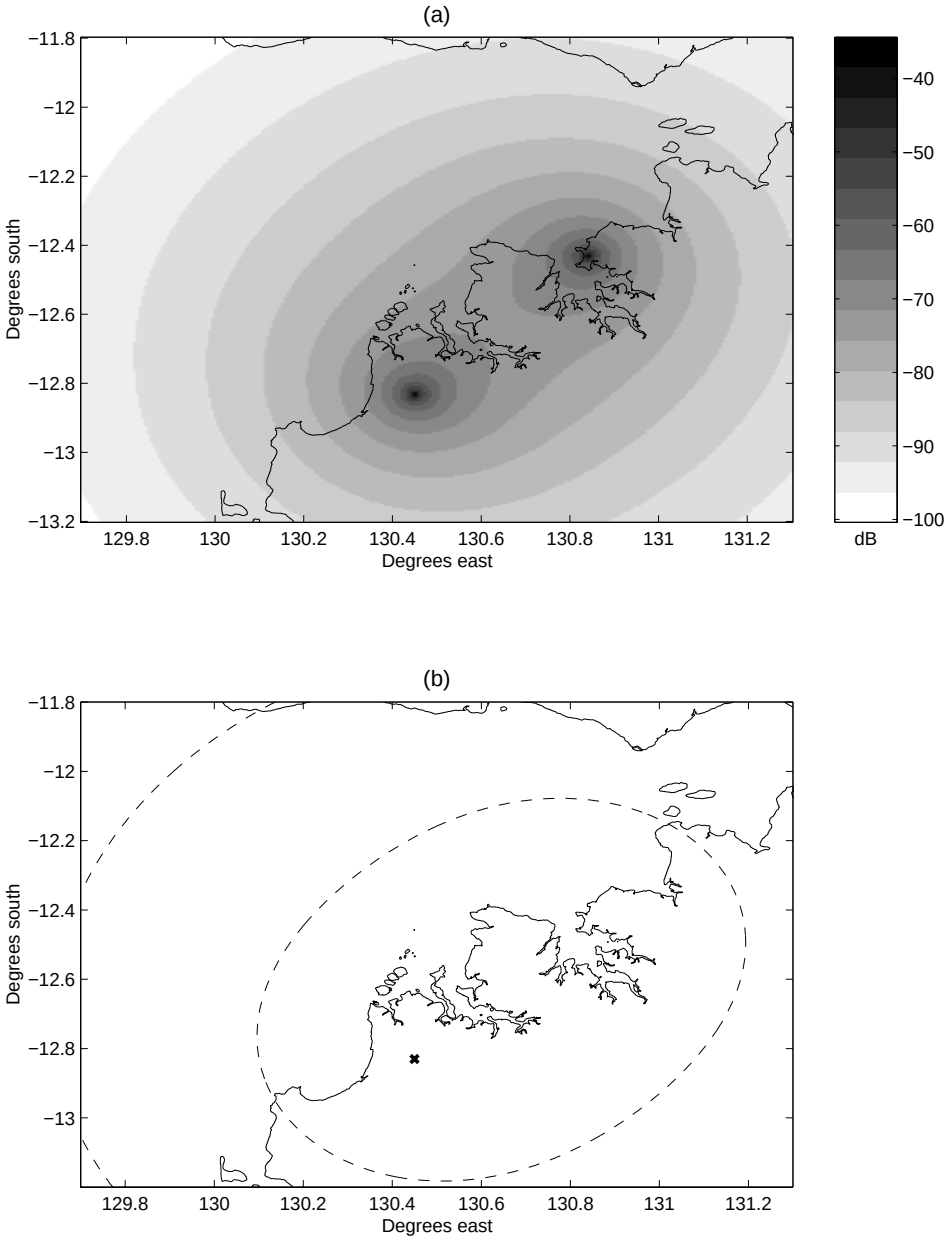

Figure 5.9: (a) Power received from the scattering from a target given its location and (b) threshold for three standard deviations above the noise floor for the first two simulations, given 50 dB attenuation towards the transmitter.

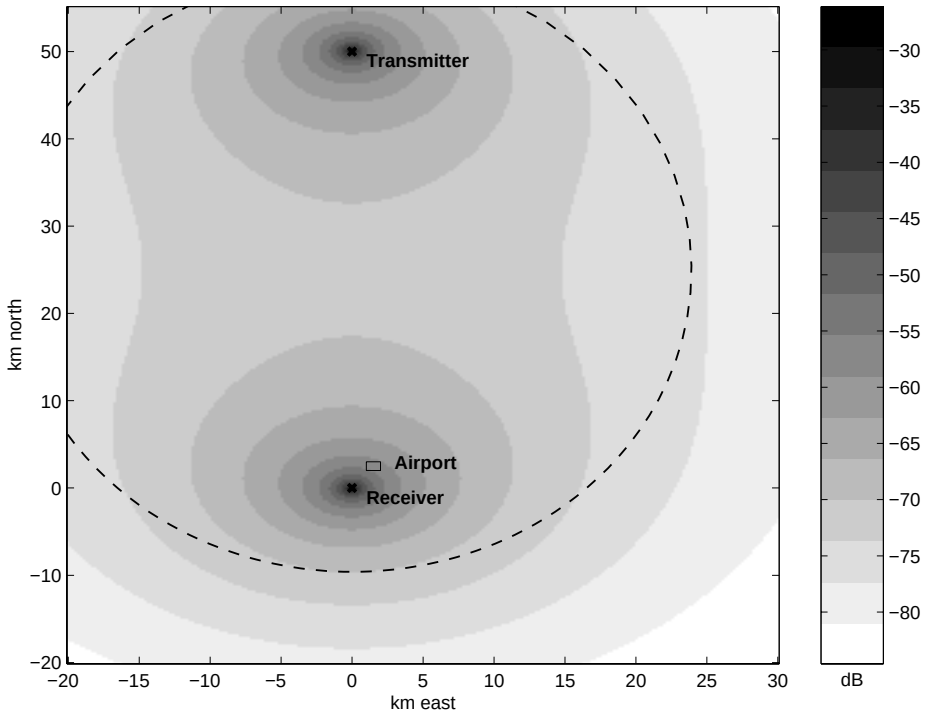

Figure 5.10: Power received from the scattering from a target given its location for the third simulation. The dashed ellipse marks a total bistatic range of 69.2 km.

is approximately $T = 1/(10^{-50/10} \times 3 \times 10^6) = 0.03$ s.

Given this integration time, the velocity resolution (length of a cell in the matched filter output along the Doppler axis) is 45 m/s=162 km/hr.

A more desirable solution to the problem of ambiguous range is to analyse the location and velocity of targets over time, as mentioned in section 3.2. Targets should vary their range over successive integration intervals as dictated by their velocity, and as integration time is small, the most likely of the possible ranges of a particular target could be estimated in a comparatively short period.

5.3 Measuring the distance to the moon

The simulations and examples provided thus far have shown how the proposed passive radar can be used to locate aircraft and ships moving relatively close to the receiver. The same techniques however, could be used to undertake a more novel project: estimating the distance to the moon. For this task, the transmitter of opportunity would be the sun.

To measure the distance to the moon, both the moon and the sun are required to be in the visible sky, so that both the direct signal and signal scattered from the moon are available to the receiver. An example of this is during the early evening when the moon is near full. The basic geometry of this experiment is illustrated in figure 5.11.

Most of the energy transmitted by the sun occurs at the frequencies corresponding to

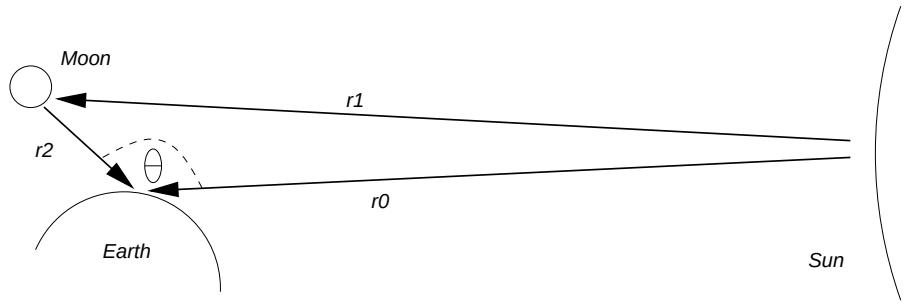

Figure 5.11: Proposed configuration for measuring the range and velocity of the moon.

visible light, although there is still much energy which occurs at lower frequencies, such as those at the high end of the radio spectrum. The U.S. National Telecommunications and Information Administration (NTIA) allocates frequencies between 250 and 252 GHz for passively monitoring radiation from space, so a carrier frequency within this band seems a reasonable choice. It is expected that the transmissions from the sun at these frequencies are very similar to white noise over realistic receiver bandwidths.

It is assumed that the distance from the earth to the sun is far greater than that from the earth to the moon, so $r_1 \approx r_0 = 149.6 \times 10^9$ m. This implies that the distance to the moon, r_2, can be simply calculated using ct_d (where t_d is the time delay of the peak in the matched filter corresponding to the return from the moon), and that an accurate measure of the angle between the direction of arrival of the two received signals, θ, is not important.

The distance to the moon is 384.4×10^6 m, and a very approximate cross-section of the moon is $\pi R_m^2 = \pi \times (3.476 \times 10^6)^2 = 38 \times 10^{12}$ m^2 (where R_m is the radius of the moon). Thus the ratio of power in the scattered signal to that in the direct signal is:

$$\begin{aligned} \frac{P_r}{P_o} &= \frac{1}{4\pi} \frac{38 \times 10^{12} \times (149.6 \times 10^9)^2}{(149.6 \times 10^9 \times 384.4 \times 10^6)^2} \\ &= 20.4 \times 10^{-6} \\ &= -47 \text{ dB} \end{aligned}$$

It is assumed that the moon is the only dominant reflector in the sky, so that if the single receiver configuration of section 3.1.2 was used, the only cross-terms would occur at $(0, 0)$ and $(-t_m, -w_m)$, where t_m and w_m are the time time delay and Doppler shift caused by the moon. Section 4.3 explains that for this configuration, the peak corresponding to the target is maximised when the attenuation towards the transmitter is such that the strength of the signal scattered from the target is equal to that of the direct signal.

Thus, it is desired that the receiver attenuate signals arriving directly from the sun by -47 dB. If this occurs, the peak in the output of the matched filter at (t_m, w_m) is 3 dB lower than the level of the peak at the origin and thus sits above the clutter floor for any reasonable time-bandwidth product.

As the amount of attenuation towards the sun varies from -47 dB, the level of the peak in the matched filter corresponding to the moon decreases, as dictated by equation (46).

For example, if the antenna was able to attenuate the direct signal by only 30 dB, the height of the peak corresponding to the moon would be:

$$\frac{|10^{(47-30)/10}|^2}{1+|10^{(47-30)/10}|^4} = 3.98 \times 10^{-4} = -34 \text{ dB}$$

The time-bandwidth product of the radar must be enough to produce a clutter floor whose level is lower than this. If a receiver with $B = 500$ kHz bandwidth was used and a signal of length $T = 4$ s was recorded, the clutter floor due to the central peak would be at -63 dB and the threshold of three standard deviations above this would correspond to -56 dB. Thus the peak revealing the time delay and Doppler shift produced by the moon would be easily detected.

The distance to the moon can be measured using a single omni-directional antenna. In this case, the peak at (t_m, w_m) would be at -97 dB. Even a small bandwidth receiver can produce a clutter pedestal lower than this if the integration time is sufficient.

Chapter 6

Conclusions

The intention of this report was to investigate the suitability of a number of broadcast band transmitters of opportunity for a passive radar. It is believed that a significant amount of work has been completed in this task.

This report has shown that signals typical of AM radio, FM radio and television broadcasting are indeed suitable radar waveforms provided that a number of other parameters of the radar are adequately tuned. These parameters are:

- The time-bandwidth product, TB (where T is the radar integration time and B is the receiver bandwidth), and
- The gain pattern of the receiver antenna

Of these, the receiver bandwidth is severely limited by the choice of transmitter of opportunity.

The most significant problem of using the proposed transmissions for passive radar is the possibility of the clutter floor due to the signal received directly from the transmitter masking the signal scattered from a target. This is controlled by ensuring the time-bandwidth product is large and by attenuating signals arriving from the direction of the transmitter.

Ideally, two receivers (and corresponding directive antenna) are required to detect targets, one collecting the direct signal and one scanning for targets in a bearing of interest. It has been shown however, that it is possible for the passive radar to operate using a single receiver (and antenna), although the performance is limited and more restrictions exist on the three parameters mentioned earlier.

Of the three types of transmissions of opportunity examined, those from FM radio appeared the most suitable as radar waveforms. These provided a signal closest to white-noise and up to a bandwidth of 75 kHz (a range resolution of up to 4 km cells).

Although this report provides a substantial investigation into the suitability of waveforms of opportunity, there exists many avenues of further study in the field. Further work includes:

- Including noise and signals scattered from the environment in the model of the received signal. In this report, it was assumed that these effects were negligible compared to the clutter due the direct transmitted signal.
- An investigation into the use of alternate detection strategies. This report has considered only applying a single threshold to the result of a matched filter, however more ad hoc algorithms may prove more successful given the particular waveforms.
- An investigation into the improvement gained by processing sequences of successive detections. This relates to tracking and is considered beyond the scope of this report.
- Analysing the transmissions of opportunity other than the three types proposed in this report. Many more surely exist, including mobile communications and satellite transmissions, which may provide more bandwidth and better self-correlation characteristics.

The most obvious continuation of the work presented in this report, however, is to physically implement the proposed passive radar.

References

1. C. E. Cook and M. Bernfeld, *Radar Signals: An Introduction to Theory and Application.* Academic Press, 1967.

2. A. W. Rihaczek, *Principles of high-resolution radar.* Peninsula Publishing, 1985.

3. F. E. Nathanson, *Radar design principles.* McGraw-Hill, 1969.

4. A. W. Rihaczek, "Radar waveform selection — a simplified approach," *IEEE Transactions on Aerospace and Electronic Systems*, vol. AES-7, pp. 1078–1086, November 1971.

5. Aerospace Publishing, "Suppression of enemy air defences," *World Aircraft Information Files*, 1998.

6. J. G. Schoenenberger and J. R. Forrest, "Principles of independent receivers for use with co-operative radar transmitters," *The Radio and Electronic Engineer*, vol. 52, pp. 93–101, February 1982.

7. M. Green, "Parasitic picture," *Electronics World*, August 1991.

8. E. C. Thompson, "Bistatic radar noncooperative illuminator synchronization techniques," *Proc. IEEE*, 1989.

9. A. Munich and E. Schecker, "Bistatic system passively tracks radar targets," *Microwaves and RF*, September 1991.

10. R. Lindop, "ESM for non cooperative bi-static radar," Tech. Rep. DSTO-RR-0096 AR-010-165, DSTO ERSL, March 1997.

11. H. D. Griffiths and N. R. W. Long, "Television based bistatic radar," *IEE Proceedings Part F*, vol. 133, pp. 649–657, December 1986.

12. H. D. Griffiths, A. J. Garnett, C. J. Baker, and S. Keaveney, "Bistatic radar using satellite-borne illuminators of opportunity," *Proceedings of the IEE International Conference on Radar*, pp. 276–279, 1992.

13. P. E. Howland, "A passive metric radar using a transmitter of opportunity," in *International Conference on Radar*, (Paris, France), Soc. Electr. and Electron., 1994.

14. J. D. Sahr and F. D. Lind, "The Manastash Ridge radar: A passive bistatic radar for upper atmosphere radio science," *Radio Science*, vol. 32, no. 6, pp. 2345–2358, 1997.

15. P. M. Woodward, *Probability and Information Theory, with Applications to Radar.* Pergamon Press, 1953.

16. D. O. North, "Analysis of factors which determine signal-to-nosie ratio discrimination in radar," tech. rep., RCA Laboratories, June 1943.

17. H. L. Van Trees, *Detection, Estimation, and Modulation Theory, Pt 3.* Wiley, 1971.

18. B. Price and E. M. Hofstetter, "Bounds on the volume and height distributions of the ambiguity function," *IEEE Transactions on Information Theory*, pp. 207–214, April 1965.

19. D. Gray, *An Introduction to Beamforming and Array Processing*. CSSIP short course notes, 1998.

20. S. Haykin, *Array Signal Processing*. Prentice–Hall, 1985.

21. B. D. O. Anderson and J. B. Moore, *Optimal Filtering*. Prentice-Hall, 1979.

22. M. I. Skolnik, *Radar Handbook*. New York: McGraw-Hill, 1970.

23. N. J. Willis, *Bistatic Radar*. Artech House, 1991.

24. A. G. Sennitt (Editor in chief), *World Radio TV Handbook*. Billboard Books, 1996.

25. L. R. Rabiner and R. W. Schafer, *Digital Processing of Speech Signals*. Prentice–Hall, 1978.

26. D. L. Cannon and G. Luecke, *Understanding Communications Systems*. Texas Instruments Learning Center, 1980.

27. B. Moran, *Detection, Estimation and Classification*. CSSIP short course notes, 1997.

28. E. Kreyszig, *Advanced Engineering Mathematics*. John Wiley & Sons, 6 ed., 1988.

Appendix A: Detail of Mathematical Analysis

A.1 Resolving range in bistatic radar

Figure 3.1 illustrates a typical bistatic radar. The direction of the main lobe of the reciever provides θ and the matched filter provides the time delay between the direct and the reflected signal, t_d, such that:

$$r_1 + r_2 - r_0 = ct_d \tag{A1}$$

where c is the speed of light. This implies:

$$\begin{aligned} r_1^2 &= (ct_d + r_0 - r_2)^2 \\ &= c^2t_d^2 + r_0^2 + r_2^2 + 2ct_dr_0 - 2ct_dr_2 - 2r_0r_2 \end{aligned} \tag{A2}$$

From the geometry of the triangle $r_0 - r_1 - r_2$ [28]:

$$r_1^2 = r_0^2 + r_2^2 - 2r_0r_2\cos\theta \tag{A3}$$

Combining equations (A2) and (A3):

$$\begin{aligned} c^2t_d^2 + 2ct_dr_0 - 2ct_dr_2 - 2r_0r_2 &= -2r_0r_2\cos\theta \\ \Rightarrow 2(ct_d + r_0 - r_0\cos\theta)r_2 &= c^2t_d^2 + 2ct_dr_0 \\ \Rightarrow r_2 &= \frac{ct_d(ct_d + 2r_0)}{2\left(ct_d + r_0(1-\cos\theta)\right)} \end{aligned} \tag{A4}$$

A.2 Resolving velocity in bistatic radar

As in the previous section, the geometry assumed in calculating the velocity of a target is shown in figure 3.1.

The matched filter provides the amount of frequency shift, w_d, between the two received signals, which relates to the rate of change of the total range of the target, $r_1 + r_2$, in the following manner:

$$\frac{d}{dt}(r_1 + r_2) = \frac{dr_1}{dt} + \frac{dr_2}{dt} = \frac{cw_d}{2\pi f_c} \tag{A5}$$

where f_c is the carrier frequency of the radar transmission.

Differentiating equation (A3) with respect to t provides:

$$r_1\frac{dr_1}{dt} - r_2\frac{dr_2}{dt} = r_0r_2\frac{d\theta}{dt}\sin\theta - r_0\cos\theta \tag{A6}$$

Solving equations (A5) and (A6) simultaineously for dr_1/dt and dr_2/dt provides the velocity of the target in the directions given by r_1 and r_2 respectively:

$$v_{r1} = \frac{dr_1}{dt} = \frac{r_2}{r_1 + r_2}\left(\frac{cw_d}{2\pi f_c} + r_0r_2\frac{d\theta}{dt}\sin\theta - r_0\cos\theta\right) \tag{A7}$$

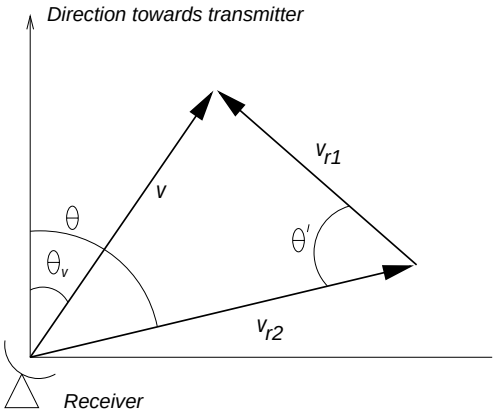

Figure A1: Geometry of the velocity of the target broken into the components along the lines r_1 and r_2.

$$v_{r2} = \frac{dr_2}{dt} = \frac{-r_1}{r_1 + r_2}\left(\frac{cw_d}{2\pi f_c} + r_0 r_2 \frac{d\theta}{dt}\sin\theta - r_0\cos\theta\right) \tag{A8}$$

Note that these equations depend on $d\theta/dt$, the rate of change of the look direction, a value which typically requires a number of radar "scans" to estimate.

The total velocity of the target is given by summing these separate components. This is illustrated in figure A1. Using similar rules of geometry that were applied in previous equations, the total target velocity, v, in the direction θ_v is:

$$v = v_{r1}^2 + v_{r2}^2 + 2v_{r1}v_{r2}\cos(\theta') \tag{A9}$$

and

$$\theta_v = \arcsin\left[\frac{v_{r1}}{v}\sin(\theta')\right] \tag{A10}$$

where θ' is the angle between r_1 and r_2 and is calculated using:

$$\theta' = \arcsin\left[\frac{r_0}{r_1}\sin\theta\right] \tag{A11}$$

A.3 Moments of the ambiguity function of white noise

Section 4.2 gives two statistical properties of the ambiguity function when the signal of interest is white Gaussian noise: the function's mean and variance. This section shows how these results were attained.

The ambiguity function for discrete signals is defined by equation (10). Properties of the model for $x[n]$ are given in section 2.2. From these, it can be shown that:

$$\begin{aligned} \mathrm{E}\{\chi(\tau,\phi)\} &= \frac{1}{N}\sum_{n=1}^{N}\mathrm{E}\{x[n]x^*[n+\tau]e^{-i\phi n}\} \\ &= \begin{cases} \sigma_x^2 & \text{for } (\tau,\phi) = (0,0) \\ 0 & \text{otherwise} \end{cases} \end{aligned}$$

and

$$\begin{aligned}
\mathrm{E}\{|\chi(\tau,\phi)|^2\} &= \frac{1}{N^2}\sum_{n_1=1}^{N}\sum_{n_2=1}^{N}\mathrm{E}\{x[n_1]x^*[n_1+\tau]e^{-i\phi n_1} \\
&\qquad (x[n_2]x^*[n_2+\tau]e^{-i\phi n_2})^*\} \\
&= \frac{1}{N^2}\sum_{n_1=1}^{N}\sum_{n_2=1}^{N}\mathrm{E}\{x[n_1]x^*[n_1+\tau]e^{-i\phi n_1}\} \\
&\qquad \mathrm{E}\{x^*[n_2]x[n_2+\tau]e^{i\phi n_2}\} \\
&\quad + \frac{1}{N^2}\sum_{n_1=1}^{N}\sum_{n_2=1}^{N}\mathrm{E}\{x[n_1]x^*[n_2]\} \\
&\qquad \mathrm{E}\{x^*[n_1+\tau]e^{-i\phi n_1}x[n_2+\tau]e^{i\phi n_2}\}
\end{aligned}$$

When $(\tau,\phi)=(0,0)$, this simplies to:

$$\begin{aligned}
\mathrm{E}\{|\chi(0,0)|^2\} &= \frac{1}{N^2}\sum_{n_1=1}^{N}\sum_{n_2=1}^{N}\sigma_x^2\sigma_x^2 + \frac{1}{N^2}\sum_{n=1}^{N}\sigma_x^2\sigma_x^2 \\
&= (1+\frac{1}{N})\sigma_x^4
\end{aligned}$$

For (τ,ϕ) pairs away from the origin:

$$\begin{aligned}
\mathrm{E}\{|\chi(\tau,\phi)|^2\} &= \frac{1}{N^2}\sum_{n_1=1}^{N}\sum_{n_2=1}^{N}0 + \frac{1}{N^2}\sum_{n=1}^{N}\sigma_x^2\sigma_x^2 \\
&= \frac{1}{N}\sigma_x^4
\end{aligned}$$

So:

$$\mathrm{E}\{|\chi(\tau,\phi)|^2\} = \begin{cases} (1+\frac{1}{N})\sigma_x^4 & \text{for } (\tau,\phi)=(0,0) \\ \frac{1}{N}\sigma_x^4 & \text{otherwise} \end{cases}$$

$$\begin{aligned}
\mathrm{E}\{|\chi(\tau,\phi)|^4\} &= \frac{1}{N^4}\sum_{n_1=1}^{N}\sum_{n_2=1}^{N}\sum_{n_3=1}^{N}\sum_{n_4=1}^{N} \\
&\qquad \mathrm{E}\{x[n_1]x^*[n_1+\tau]e^{-i\phi n_1}x[n_2+\tau]e^{i\phi n_2}x^*[n_2] \\
&\qquad x[n_3]x^*[n_3+\tau]e^{-i\phi n_3}x[n_4+\tau]e^{i\phi n_1}x^*[n_4]\} \\
&= \frac{1}{N^4}\sum_{n_1=1}^{N}\sum_{n_2=1}^{N}\sum_{n_3=1}^{N}\sum_{n_4=1}^{N} \\
&\qquad \Big(\mathrm{E}\{x[n_1]x^*[n_1+\tau]e^{-i\phi n_1}\}\mathrm{E}\{x[n_2+\tau]e^{i\phi n_2}x^*[n_2]\} \\
&\qquad \mathrm{E}\{x[n_3]x^*[n_3+\tau]e^{-i\phi n_3}\}\mathrm{E}\{x[n_4+\tau]e^{i\phi n_1}x^*[n_4]\} \\
&\qquad + \mathrm{E}\{x[n_1]x^*[n_1+\tau]e^{-i\phi n_1}\}\mathrm{E}\{x[n_2+\tau]e^{i\phi n_2}x^*[n_2]\}
\end{aligned}$$

$$
\begin{aligned}
&\mathrm{E}\{x[n_3]x^*[n_4]\}\mathrm{E}\{x[n_4+\tau]e^{i\phi n_1}x^*[n_3+\tau]e^{-i\phi n_3}\}\\
&+\mathrm{E}\{x[n_1]x^*[n_1+\tau]e^{-i\phi n_1}\}\mathrm{E}\{x[n_4+\tau]e^{i\phi n_1}x^*[n_4]\}\\
&\mathrm{E}\{x[n_3]x^*[n_2]\}\mathrm{E}\{x[n_2+\tau]e^{i\phi n_2}x^*[n_3+\tau]e^{-i\phi n_3}\}\\
&+\mathrm{E}\{x[n_1]x^*[n_1+\tau]e^{-i\phi n_1}\}\mathrm{E}\{x[n_4+\tau]e^{i\phi n_1}x^*[n_2]\}\\
&\mathrm{E}\{x[n_3]x^*[n_4]\}\mathrm{E}\{x[n_2+\tau]e^{i\phi n_2}x^*[n_3+\tau]e^{-i\phi n_3}\}\\
&+\mathrm{E}\{x[n_1]x^*[n_1+\tau]e^{-i\phi n_1}\}\mathrm{E}\{x[n_2+\tau]e^{i\phi n_2}x^*[n_4]\}\\
&\mathrm{E}\{x[n_3]x^*[n_2]\}\mathrm{E}\{x[n_4+\tau]e^{i\phi n_1}x^*[n_3+\tau]e^{-i\phi n_3}\}\\
&+\mathrm{E}\{x[n_1]x^*[n_1+\tau]e^{-i\phi n_1}\}\mathrm{E}\{x[n_2+\tau]e^{i\phi n_2}x^*[n_4]\}\\
&\mathrm{E}\{x[n_3]x^*[n_3+\tau]e^{-i\phi n_3}\}\mathrm{E}\{x[n_4+\tau]e^{i\phi n_1}x^*[n_2]\}\\
&+\mathrm{E}\{x[n_1]x^*[n_2]\}\mathrm{E}\{x[n_2+\tau]e^{i\phi n_2}x^*[n_1+\tau]e^{-i\phi n_1}\}\\
&\mathrm{E}\{x[n_3]x^*[n_3+\tau]e^{-i\phi n_3}\}\mathrm{E}\{x[n_4+\tau]e^{i\phi n_1}x^*[n_4]\}\\
&+\mathrm{E}\{x[n_1]x^*[n_2]\}\mathrm{E}\{x[n_2+\tau]e^{i\phi n_2}x^*[n_1+\tau]e^{-i\phi n_1}\}\\
&\mathrm{E}\{x[n_3]x^*[n_4]\}\mathrm{E}\{x[n_4+\tau]e^{i\phi n_1}x^*[n_3+\tau]e^{-i\phi n_3}\}\\
&+\mathrm{E}\{x[n_1]x^*[n_2]\}\mathrm{E}\{x[n_2+\tau]e^{i\phi n_2}x^*[n_3+\tau]e^{-i\phi n_3}\}\\
&\mathrm{E}\{x[n_3]x^*[n_1+\tau]e^{-i\phi n_1}\}\mathrm{E}\{x[n_4+\tau]e^{i\phi n_1}x^*[n_4]\}\\
&+\mathrm{E}\{x[n_1]x^*[n_2]\}\mathrm{E}\{x[n_2+\tau]e^{i\phi n_2}x^*[n_3+\tau]e^{-i\phi n_3}\}\\
&\mathrm{E}\{x[n_3]x^*[n_4]\}\mathrm{E}\{x[n_4+\tau]e^{i\phi n_1}x^*[n_1+\tau]e^{-i\phi n_1}\}\\
&+\mathrm{E}\{x[n_1]x^*[n_2]\}\mathrm{E}\{x[n_4+\tau]e^{i\phi n_1}x^*[n_3+\tau]e^{-i\phi n_3}\}\\
&\mathrm{E}\{x[n_3]x^*[n_1+\tau]e^{-i\phi n_1}\}\mathrm{E}\{x[n_2+\tau]e^{i\phi n_2}x^*[n_4]\}\\
&+\mathrm{E}\{x[n_1]x^*[n_2]\}\mathrm{E}\{x[n_4+\tau]e^{i\phi n_1}x^*[n_1+\tau]e^{-i\phi n_1}\}\\
&\mathrm{E}\{x[n_3]x^*[n_3+\tau]e^{-i\phi n_3}\}\mathrm{E}\{x[n_2+\tau]e^{i\phi n_2}x^*[n_4]\}\\
&+\mathrm{E}\{x[n_1]x^*[n_3+\tau]e^{-i\phi n_3}\}\mathrm{E}\{x[n_4+\tau]e^{i\phi n_1}x^*[n_4]\}\\
&\mathrm{E}\{x[n_3]x^*[n_2]\}\mathrm{E}\{x[n_2+\tau]e^{i\phi n_2}x^*[n_1+\tau]e^{-i\phi n_1}\}\\
&+\mathrm{E}\{x[n_1]x^*[n_3+\tau]e^{-i\phi n_3}\}\mathrm{E}\{x[n_4+\tau]e^{i\phi n_1}x^*[n_2]\}\\
&\mathrm{E}\{x[n_3]x^*[n_4]\}\mathrm{E}\{x[n_2+\tau]e^{i\phi n_2}x^*[n_1+\tau]e^{-i\phi n_1}\}\\
&+\mathrm{E}\{x[n_1]x^*[n_3+\tau]e^{-i\phi n_3}\}\mathrm{E}\{x[n_2+\tau]e^{i\phi n_2}x^*[n_2]\}\\
&\mathrm{E}\{x[n_3]x^*[n_1+\tau]e^{-i\phi n_1}\}\mathrm{E}\{x[n_4+\tau]e^{i\phi n_1}x^*[n_4]\}\\
&+\mathrm{E}\{x[n_1]x^*[n_3+\tau]e^{-i\phi n_3}\}\mathrm{E}\{x[n_2+\tau]e^{i\phi n_2}x^*[n_2]\}\\
&\mathrm{E}\{x[n_3]x^*[n_4]\}\mathrm{E}\{x[n_4+\tau]e^{i\phi n_1}x^*[n_1+\tau]e^{-i\phi n_1}\}\\
&+\mathrm{E}\{x[n_1]x^*[n_3+\tau]e^{-i\phi n_3}\}\mathrm{E}\{x[n_2+\tau]e^{i\phi n_2}x^*[n_4]\}\\
&\mathrm{E}\{x[n_3]x^*[n_1+\tau]e^{-i\phi n_1}\}\mathrm{E}\{x[n_4+\tau]e^{i\phi n_1}x^*[n_2]\}\\
&+\mathrm{E}\{x[n_1]x^*[n_3+\tau]e^{-i\phi n_3}\}\mathrm{E}\{x[n_2+\tau]e^{i\phi n_2}x^*[n_4]\}\\
&\mathrm{E}\{x[n_3]x^*[n_2]\}\mathrm{E}\{x[n_4+\tau]e^{i\phi n_1}x^*[n_1+\tau]e^{-i\phi n_1}\}\\
&+\mathrm{E}\{x[n_1]x^*[n_4]\}\mathrm{E}\{x[n_2+\tau]e^{i\phi n_2}x^*[n_1+\tau]e^{-i\phi n_1}\}\\
&\mathrm{E}\{x[n_3]x^*[n_2]\}\mathrm{E}\{x[n_4+\tau]e^{i\phi n_1}x^*[n_3+\tau]e^{-i\phi n_3}\}\\
&+\mathrm{E}\{x[n_1]x^*[n_4]\}\mathrm{E}\{x[n_2+\tau]e^{i\phi n_2}x^*[n_1+\tau]e^{-i\phi n_1}\}\\
&\mathrm{E}\{x[n_3]x^*[n_3+\tau]e^{-i\phi n_3}\}\mathrm{E}\{x[n_4+\tau]e^{i\phi n_1}x^*[n_2]\}\\
&+\mathrm{E}\{x[n_1]x^*[n_4]\}\mathrm{E}\{x[n_4+\tau]e^{i\phi n_1}x^*[n_3+\tau]e^{-i\phi n_3}\}
\end{aligned}
$$

$$
\begin{aligned}
&\mathrm{E}\{x[n_3]x^*[n_1+\tau]e^{-i\phi n_1}\}\mathrm{E}\{x[n_2+\tau]e^{i\phi n_2}x^*[n_2]\}\\
&+\mathrm{E}\{x[n_1]x^*[n_4]\}\mathrm{E}\{x[n_4+\tau]e^{i\phi n_1}x^*[n_1+\tau]e^{-i\phi n_1}\}\\
&\mathrm{E}\{x[n_3]x^*[n_3+\tau]e^{-i\phi n_3}\}Ex[n_2+\tau]e^{i\phi n_2}x^*[n_2]\\
&+\mathrm{E}\{x[n_1]x^*[n_4]\}\mathrm{E}\{x[n_2+\tau]e^{i\phi n_2}x^*[n_3+\tau]e^{-i\phi n_3}\}\\
&\mathrm{E}\{x[n_3]x^*[n_1+\tau]e^{-i\phi n_1}\}\mathrm{E}\{x[n_4+\tau]e^{i\phi n_1}x^*[n_2]\}\\
&+\mathrm{E}\{x[n_1]x^*[n_4]\}\mathrm{E}\{x[n_2+\tau]e^{i\phi n_2}x^*[n_3+\tau]e^{-i\phi n_3}\}\\
&\mathrm{E}\{x[n_3]x^*[n_2]\}\mathrm{E}\{x[n_4+\tau]e^{i\phi n_1}x^*[n_1+\tau]e^{-i\phi n_1}\}\Big)
\end{aligned}
$$

When $(\tau,\phi)=(0,0)$, this simplies to:

$$\mathrm{E}\{|\chi(0,0)|^4\} \quad = \quad \frac{1}{N^4}\sigma_x^8(N^4+6N^3+8N^2+9N)$$

And for (τ,ϕ) pairs away from the origin:

$$\mathrm{E}\{|\chi(\tau,\phi)|^4\} \quad = \quad \frac{1}{N^4}\sigma_x^8(3N^2+6N)$$

So:

$$\mathrm{E}\{|\chi(\tau,\phi)|^4\} = \begin{cases} (1+\frac{6}{N}+\frac{8}{N^2}+\frac{9}{N^3})\sigma_x^8 & \text{for } \tau=\phi=0 \\ (\frac{3}{N^2}+\frac{6}{N^3})\sigma_x^8 & \text{otherwise} \end{cases}$$

Appendix B: Matlab Code

Two equations which were commonly referenced throughout this report were equations (6) and (10), which calculated the matched filter output and the ambiguity function respectively. This appendix provides Matlab code which implements these equations.

It is worth noting that these functions are very similar. This is not surprising given the similarity of the equations and that both operations are effectively correlating one signal with another delayed in time and shifted in Doppler.

B.1 Matched filter receiver

```
function M = match(xr,xt,fs,tau,phi,win)
% Matched filter radar receiver
%
% M = MATCH(xr,xt,fs,tau,phi,win)
%
% xr  : Received signal.
% xt  : Transmitted signal. This must be the same length
%       as xr.
% fs  : Sampling frequency of xr and xt (in Hz).
% tau : Vector of time delays (in secs) at which to
%       evaluate the matched filter.
%       This should be an evenly spaced vector with the
%       spacing between elements being a multiple of 1/fs.
%       If tau is the empty matrix, or is not specified,
%       the default is [0:1/fs:length(xr)/fs].
% phi : Vector of frequency shifts (in Hz) at which to
%       evaluate the matched filter.
%       If phi is the empty matrix, or is not specified,
%       the default is [-fs:fs/50:fs].
% win : What window function is used when processing.
%       If not specified or is the empty matrix, no window
%       (effective rectangular or boxcar window) is used.
%       If win is a vector of the same length as xr and xt,
%       it is used as the window function.
%       win can be one of the following strings, in which
%       case the window function is calculated and used:
%       'hanning', 'hamming', 'blackman', 'boxcar'
%
% The result of the matched filter, M, is a matrix of
% length(tau) rows and length(phi) columns.  The rows
% correspond to the possibility of targets at the various
% ranges which (through the bandwidth used and radar
% configuration) correspond to the values in tau.  The
```

```
% columns correspond to the radial velocity of these targets
% which correspond to the frequency shifts phi.
%
% Example of use:
%   fs = 1280;
%   xt = sin(2*pi*55*[0:1/fs:127/fs]);
%   xr = [zeros(1,10) xt(1:118)];
%   tau = [0:1/fs:20/fs];
%   phi = [-fs/2:fs/4:fs/2];
%   M = match(xr,xt,fs,tau,phi);
%   mesh(phi,tau,M), axis tight
%
% By Maurice Ringer, 1998

error(nargchk(3,6,nargin));

nx = length(xr);
if nx~=length(xt)
  error('xt and xr must be the same length')
end

if nargin<4, tau = []; end
if nargin<5, phi = []; end
if nargin<6, win = []; end

if isempty(tau), tau = [0:1/fs:nx/fs]; end
if isempty(phi), phi = [-fs:fs/50:fs]; end
if isempty(win), win = ones(nx,1);     end
if isstr(win)
  win = lower(win);
  if strcmp(win,'hanning')
    win = 0.5*(1 - cos(2*pi*[1:nx]'/(nx+1)));
  elseif strcmp(win,'hamming')
    win = 0.54 - 0.46*cos(2*pi*[0:nx-1]'/(nx-1));
  elseif strcmp(win,'blackman')
    win = (0.42 - 0.5*cos(2*pi*(0:nx-1)/(nx-1)) + ...
      0.08*cos(4*pi*(0:nx-1)/(nx-1)))';
  elseif strcmp(win,'boxcar')
    win = ones(nx,1);
  else
    warning('Funny window argument - no window used');
    win = ones(nx,1);
  end
end

ntau = length(tau);
nphi = length(phi);
```

```
xr = xr(:).*win;
xt = xt(:).*win;
phi = phi(:);

M = zeros(ntau,nphi);
for itau = 1:ntau,
  n = round(tau(itau)*fs);
  if (abs(n)<nx)
    if (n>=0)
      temp = xr(1+n:nx) .* conj(xt(1:nx-n));
      t = [n/fs:1/fs:(nx-1)/fs];
    else
      temp = xr(1:nx+n) .* conj(xt(1-n:nx));
      t = [0:1/fs:(nx+n-1)/fs];
    end
    M(itau,:) = (exp(-i*2*pi*phi*t) * temp).';
  end
end

M = abs(M).^2;
M = M / max(max(M));
```

B.2 Ambiguity function generation

```
function X = amb(z,t,tau,nu);
% Radar Ambiguity function
%
% X = AMB(z,t,tau,phi)
%
% z   : Analytic input signal. Values for z outside time t are
%       assummed to be zero.
% t   : Timebase for the input signal (in seconds). This must
%       be a vector of equally spaced numbers.
% tau : Vector of time delays (in seconds) to evaluate X at
% phi  : Vector of Doppler shifts (in Hz) to evaluate X at
%
% X   : Resulting radar ambiguity function. This is a real
%       matrix of size (length(tau),length(phi))
%
% Example of use:
%   t = [0:63]'; z = exp(i*2*pi*4/64*t);
%   tau = [-64:4:64]'; phi = [-0.16:0.016:0.16]';
%   X = amb(z,t,tau,phi);
%   surf(phi,tau,10*log10(X)); axis tight;
```

```
%
% This code implements equation 4-2a (pg 59), from
% "Radar Signals: An Introduction to Theory and Application"
% by C E Cook and M Bernfeld, 1967, Academic Press
%
% Maurice Ringer, 1998

error(nargchk(4,4,nargin));

z = z(:);
t = t(:);
tau = tau(:);
phi = phi(:);
t_sp = t(2) - t(1);

nt = length(t);
ntau = length(tau);
nphi = length(phi);

if nt~=length(z)
  error('length of arguments z and t must be the same');
end

X = zeros(ntau,nphi);
for itau = 1:ntau,
  n = round(tau(itau)/t_sp);
  if (abs(n)<nt)
    if (n>=0)
      temp = z(1:nt-n) .* conj(z(n+1:nt));
      X(itau,:) = temp.' * exp(-i*2*pi*t(1:nt-n)*phi');
    else
      temp = z(-n+1:nt) .* conj(z(1:nt+n));
      X(itau,:) = temp.' * exp(-i*2*pi*t(-n+1:nt)*phi');
    end
  end
end

X = abs(X).^2;
X = X / max(max(X));
```

DISTRIBUTION LIST

Waveform Analysis of Transmitters of Opportunity for Passive Radar

M A Ringer, G J Frazer and S J Anderson

	Number of Copies
DEFENCE ORGANISATION	
Task Sponsor	
Chief, Surveillance Systems Division	1
S&T Program	
Chief Defence Scientist FAS Science Policy AS Science Corporate Management	1
Director General Science Policy Development	1
Counsellor, Defence Science, London	Doc Data Sht
Counsellor, Defence Science, Washington	Doc Data Sht
Scientific Adviser Policy and Command	1
Navy Scientific Adviser	Doc Data Sht
Scientific Adviser, Army	Doc Data Sht
Air Force Scientific Adviser	1
Director Trials	1
Electronics and Surveillance Research Laboratory	
Director, Electronics and Surveillance Research Laboratory	1
Surveillance Systems Division	
Research Leader, Wide Area Surveillance Branch	1
Head, Radar Signal Processing Group	1
Maurice A. Ringer	4
Dr. Gordon J. Frazer	3
Dr. Stuart J. Anderson	3
DSTO Libraries and Archives	
Library Fishermens Bend	1
Library Maribyrnong	1
Library Salisbury	2
Library Sydney	Doc Data Sht
Australian Archives	1
US Defense Technical Information Center	2
UK Defence Research Information Centre	2
Canada Defence Scientific Information Service	1

NZ Defence Information Centre	1
National Library of Australia	1
Capability Development Division	
Director General Maritime Development	Doc Data Sht
Director General Aerospace Development	Doc Data Sht
Director General Land Development	Doc Data Sht
Director General C3I Development	Doc Data Sht
Intelligence Program	
Defence Intelligence Organisation	1
Director, Electronics Section	1
Corporate Support Program (libraries)	
Officer in Charge, TRS, Defence Regional Library, Canberra	1

UNIVERSITIES AND COLLEGES

Australian Defence Force Academy	
Library	1
Head of Aerospace and Mechanical Engineering	1
Serials Section (M list), Deakin University Library, Geelong	1
Senior Librarian, Hargrave Library, Monash University	1
Librarian, Flinders University	1

OTHER ORGANISATIONS

NASA (Canberra)	1
AGPS	1
State Library of South Australia	1
Parliamentary Library, South Australia	1

ABSTRACTING AND INFORMATION ORGANSISATIONS

Library, Chemical Abstracts Reference Service	1
Engineering Societies Library, US	1
Materials Information, Cambridge Scientific Abstracts, US	1
Documents Librarian, The Center for Research Libraries, US	1

INFORMATION EXCHANGE AGREEMENT PARTNERS

Aquisitions Unit, Science Reference and Information Service, UK	1
Library - Exchange Desk, National Institute of Standards and Technology, US	1

SPARES

DSTO Salisbury Research Library	6
Total number of copies:	55

DEFENCE SCIENCE AND TECHNOLOGY ORGANISATION DOCUMENT CONTROL DATA	1. CAVEAT/PRIVACY MARKING

2. TITLE	3. SECURITY CLASSIFICATION
Waveform Analysis of Transmitters of Opportunity for Passive Radar	Document (U) Title (U) Abstract (U)
4. AUTHOR(S)	5. CORPORATE AUTHOR
M A Ringer, G J Frazer and S J Anderson	Electronics and Surveillance Research Laboratory PO Box 1500 Salisbury, South Australia, Australia 5108

6a. DSTO NUMBER	6b. AR NUMBER	6c. TYPE OF REPORT	7. DOCUMENT DATE
DSTO–TR–0809	010–901	Technical Report	June, 1999

8. FILE NUMBER	9. TASK NUMBER	10. SPONSOR	11. No OF PAGES	12. No OF REFS
9505/017/0023/01	DST 97/006		71	28

13. DOWNGRADING / DELIMITING INSTRUCTIONS	14. RELEASE AUTHORITY
Not Applicable	Chief, Surveillance Systems Division

15. SECONDARY RELEASE STATEMENT OF THIS DOCUMENT

Approved For Public Release

OVERSEAS ENQUIRIES OUTSIDE STATED LIMITATIONS SHOULD BE REFERRED THROUGH DOCUMENT EXCHANGE, PO BOX 1500, SALISBURY, SOUTH AUSTRALIA 5108

16. DELIBERATE ANNOUNCEMENT

No Limitations

17. CITATION IN OTHER DOCUMENTS

No Limitations

18. DEFTEST DESCRIPTORS

Passive detection	Waveforms
Matched filters	Radar transmitters

19. ABSTRACT

This report investigates the suitability of a number of broadcast band transmitters of opportunity for a passive radar. Specifically, this report reviews the design of active radar waveforms, measures emissions for representative transmitters of opportunity, and assesses the suitability of these signals for various types of radar observation.

This report shows that it is indeed possible to construct the suggested passive radar, although performance is limited and depends largely on other parameters, such as receiver bandwidth, antenna pattern and observation time.